

Know Unreported Roadway Incidents in Real-time: A Deep Learning Framework for Early Traffic Anomaly Detection

Haocheng Duan^a, Hao Wu^a, Sean Qian^{ab*}

^aDepartment of Civil and Environmental Engineering, Carnegie Mellon University

^bHeinz College, Carnegie Mellon University

*Corresponding author: Sean Qian; seanqian@cmu.edu

Abstract

The goal of this research is to know traffic anomalies as early as possible. A traffic anomaly refers to a generic incident on the road that influences traffic flow and calls for urgent traffic management measures. “Knowing” the occurrence of a traffic anomaly is twofold: the ability to detect this anomaly before it is reported anywhere, or it may be such that an anomaly can be predicted before it actually occurs on the road (e.g., non-recurrent traffic breakdown). Either way, the objective is to inform traffic operators of unreported incidents in real time (and as early as possible), regardless of whether it is being reported later or not. The key is to stay ahead of the curve. Time is of the essence.

Conventional automatic incident detection (AID) has relied heavily on all incident reports exclusively for training and evaluation. However, these reports suffer from a number of issues, such as delayed reports, inaccurate descriptions, false alarms, missing reports, and incidents that do not necessarily influence traffic. Relying on these reports to train or calibrate AID models hinders their ability to detect traffic anomalies effectively and timely, even leading to convergence issues in the model training process. Moreover, conventional AID models are not inherently designed to capture the early indicators of any generic incidents. It remains unclear how far ahead an AID model can report incidents. The AID applications in the literature are also spatially limited because the data used by most models is often limited to specific test road segments. To solve these problems, we propose a deep learning framework utilizing prior domain knowledge and model-designing strategies. This allows the model to detect a broader range of anomalies, not only incidents that significantly influence traffic flow but also early characteristics of incidents along with historically unreported anomalies. We specially design the model to target the early-stage detection/prediction of an incident. Additionally, unlike most conventional AID studies, we use widely available data, enhancing our method’s scalability. The experimental results across numerous road segments on different maps demonstrate that our model leads to more effective and early anomaly detection. Our framework does not focus on stacking or tweaking various deep learning models; instead, it focuses on model design and training strategies to improve early detection performance.

Keywords: Automatic Incident Detection, Non-recurrent Traffic, Anomaly Detection, Incident Management

1 Introduction

Traffic congestion grievously disrupts the everyday lives of urban residents and causes substantial economic losses. It can be categorized into recurring and non-recurring congestion. Recurring congestion occurs periodically when traffic volume exceeds the road’s capacity. In contrast, non-recurring congestion, also known as *traffic anomalies*, is caused by incidents such as crashes, work zones, and special events. In the U.S., non-recurring congestion accounts for over half of the total congestion ([Federal Highway Administration \(FHWA\), 2020b](#)). Mitigating non-recurring impacts requires accurately knowing roadway incidents in advance and proactive management strategies as opposed to being reactive. Figure 1 illustrates the FHWA timeline for managing non-recurring events, highlighting that the effectiveness of proactive strategies heavily relies on the timely detection and verification of incidents. However, incident reports in the real world are typically delayed and subject to multiple layers of verification, not to mention a large number of unreported incidents. Acknowledging that incident reports are oftentimes late or missing, traffic operators may find their actions too late by the time they are informed of non-recurrent congestion. To assist traffic operators in implementing real-time control measures ([F. Ahmed & Hawas, 2015](#); [Z. Ke, Zou, et al., 2024](#); [Sheu, 2002](#)) and travelers in

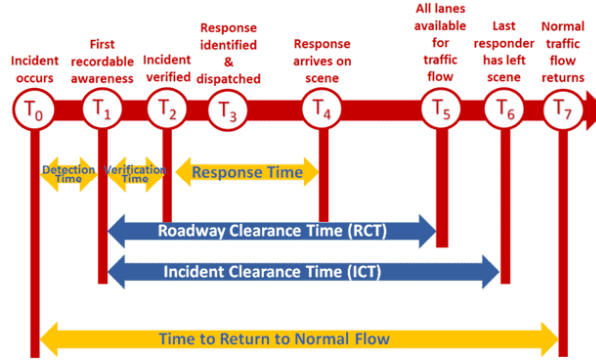


Figure 1: Incident Management Timeline (Federal Highway Administration (FHWA), 2020a)

planning their journeys (Z. Ke, Duan, & Qian, 2024; Xie et al., 2020), it is crucial to verify incident reports more promptly, or better yet, detect incidents before they are reported and effectively identify unreported incidents. Our goal is to alert traffic operators of an anomaly before T_1 , the current practice, by as much as we can, and ideally even before T_0 referred in Figure 1.

Conventional automatic incident detection (AID) methods may assist in verifying incident reports, but it is unclear if AID is able to detect incidents earlier than the reports themselves *after the fact* and efficiently identify unreported incidents. This is because they are typically tuned/trained and evaluated based solely on all incident reports, thereby inheriting the same delays and missing issues. These issues will be further discussed in detail later in this section. This paper aims to overcome the bottlenecks caused by incident reports in conventional AID methods and management strategies, with the goal of detecting or predicting anomalies as early as possible. Here, we use “early anomaly detection” to indicate that our problem is fundamentally different from conventional AID and from network traffic speed/counts prediction. An anomaly in this paper is defined not only as a reported incident but also as any incident that may not be reported at the time, potentially reported later, or not reported at all, yet significantly impacts traffic flow in the near term. Efficiently detecting all these anomalies, especially unreported incidents and incidents that have not yet been reported, is essential for the timely implementation of proactive control measures and the overall incident management process.

Given the exact anomaly occurrence time (namely T_0 referred in Figure 1) is usually unknown in practice, we do not necessarily differentiate “detecting” an ongoing but unreported anomaly and “predicting” an anomaly that has not occurred yet. The goal is to know an unreported anomaly in advance, regardless of whether it has occurred. It is critical to clarify we do not intend to “predict” the occurrence of an incident before it actually occurs, since generally incident occurrence is rare and random. Our intention is to know the anomaly as early as we can, even if there is very little sign of an incident yet. This means that at the time of anomaly detection, it is likely an incident has occurred, but not reported anywhere (including Waze and social media, which is considered more timely than other traditional manners). It is also possible (but unlikely) an incident may not have occurred, but a certain traffic/weather condition may lead to high risks resulting its occurrence in the near future. Again, our algorithm does not differentiate this “detection” or “prediction” nature, thus lending its name to “early anomaly detection”. We also do not intend to detect or predict the attributes of an incident, its type, duration, etc.

Conventional AID methods struggle with early anomaly detection. Over the decades, AID has evolved from traditional statistical and comparative approaches to AI-driven methods. However, regardless of the technique used, these methods rely on mining differences in traffic states with and without incidents. Incident reports, being the most intuitive reference for incidents, thus are almost universally used to calibrate or train AID models. Yet, incident reports are not equivalent to anomalies. Real-world incident reports often contain numerous false positives, inaccurate information, or incidents that do not impact traffic conditions. Directly using them to calibrate models can introduce significant bias and even lead to convergence issues during model training. Therefore, existing research often involves manual review (Abdulhai & Ritchie, 1999; Dia & Rose, 1997; Jin et al., 2002) and even camera calibration (Chakraborty et al., 2019) to filter out false or insignificant reports. This approach is neither feasible for scaling nor capable of addressing other significant inherent issues, especially delays and missing.

The issue of delayed incident report arises from the long reaction time between the incident occurrence and when they are reported (ElSahly & Abdelfatah, 2022; Gu et al., 2016). Figure 2 illustrates the delay of incident reports by displaying the relationship between Waze reports and speed on an I-70 highway segment in Howard County, MD. The blue line represents the speed on the day of the incident report, while the other dotted lines represent the speed on the same days of the week and at the same time, providing a recurrent reference. It can be seen from the figure that Waze incident reports are significantly delayed compared to the impact on speed.

As a result of overlooking delays in incident reports, those features prior to incident reports are often missing from training an AID model. Due to the lack of training samples in the early stage of an incident, the model is unable to learn from these features signaling an upcoming or ongoing incident, hindering timely detection. It is worth noting that many studies emphasize achieving near-zero mean time to detection (MTTD) as evidence of timely detection:

$$\text{MTTD} = \frac{\sum_{i=1}^{N_{\text{detected}}} (t_i^{\text{alarm}} - t_i^{\text{report}})}{N_{\text{detected}}} \quad (1)$$

where N_{detected} refers to the number of incident reports being detected, t_i^{report} refers to the start time of the report, and t_i^{alarm} refers to the time when the model begins to trigger an alert. However, this is because their evaluation process compares detection times to delayed incident reports, so a near-zero MTTD simply indicates that the alarm is triggered shortly after the incident is reported, not when it actually occurs.

In addition, the issue of missing incident reports is mainly because incident reports still largely rely on either fixed location sensors that are extremely limited or passing drivers to report actively (e.g. Waze, X, etc.). In fact, many incidents or traffic anomalies go unreported (Turner et al., 2015). Figure 3 illustrates examples of significant anomalies that were not reported on the same segment as in Figure 2. The blue line highlights anomalies without corresponding incident reports during those times, while the other dashed lines represent the speed on the same days of the week and at the same time, providing a recurrent reference. Significant anomalies can be observed even without the presence of an incident report. Those data under unreported anomalies are otherwise not included in the incident detection/prediction models. Even worse, they are labeled as data under recurrent traffic conditions, which could mislead the training of AID models.

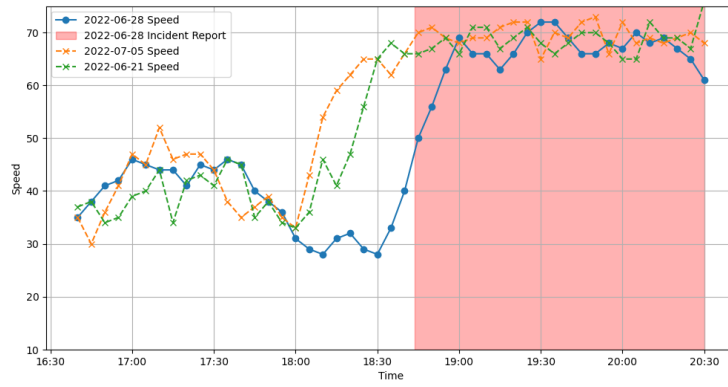
In summary, overlooking the issues related to incident reports leads existing AID methods to fit their results to the reports themselves (which may be delayed, false, or missing) rather than to true and timely anomalies, particularly the early stages of an incident or unreported incidents, limiting conventional AID models' performance.

Besides performance issues, another key challenge for conventional AID methods today is their scalability and generalizability. Most of the data used in AID methods, such as loop detector data, traffic camera data, and high-precision GPS data, are not widely available or can be very costly in real-time. For instance, real-time 24/7 loop detector data is limited to a very small number of segments or none in most regions. Social media data used by a few studies have also faced more scraping restrictions nowadays. On the other hand, data sources such as INRIX (www.inrix.com), HERE (www.here.com), and TomTom (www.tomtom.com) provide probe vehicle speed data, while Waze (www.waze.com) and State DOT offer incident reports. These data sources cover almost all major roads, providing the foundation for large-scale generalization of AID methods. The more ubiquitous data coverage of spaces and time enables a better understanding of network traffic flow and, thus, early anomaly detection on most road segments. It is essential to develop an incident detection/prediction model relying on those data so that we can afford to detect/predict incidents virtually anywhere and anytime. However, very few models are built exclusively on such data.

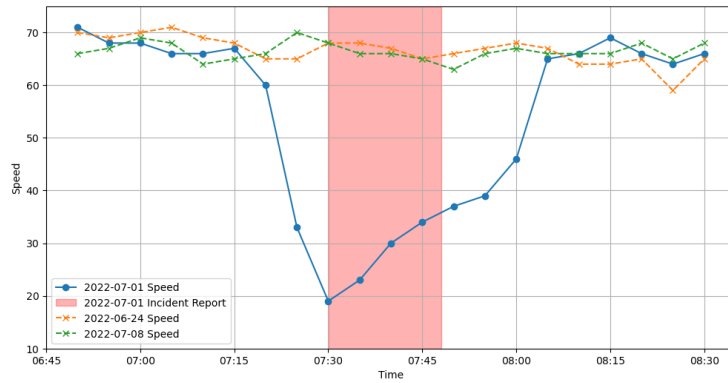
To address the above problems, we will propose an early anomaly detection system that can learn and capture a wider range of anomalies, i.e., not only fits incident reports but also detects early incident features and unreported anomalies, enhancing the model's practical significance. In addition, to ensure scalability and generalizability, the inputs to the new model should be limited to widely available low-cost data rather than data from extremely selected locations. Our contributions can be summarized as:

- We propose an early anomaly detection model employing several training and model design strategies. Our model not only aligns well with true incident reports but also performs early detection or prediction of incidents before they are reported later *after the fact* or not reported at all. This model is fundamentally different from conventional AID models.
- In contrast to most datasets in the literature, our method does not require manual selection of anomaly reports during training, saving a significant amount of manpower and increasing its scalability.
- Our model uses ubiquitously available and low-cost data, increasing its scalability and generalizability. Unlike most existing studies that test one or two specifically selected segments, we conducted experiments on ten segments across two road networks, which can be generalized to any size of road segments in the network.
- Even with low-cost data, our model effectively balances the detection rate and false alarm rate, outperforming the baseline models.

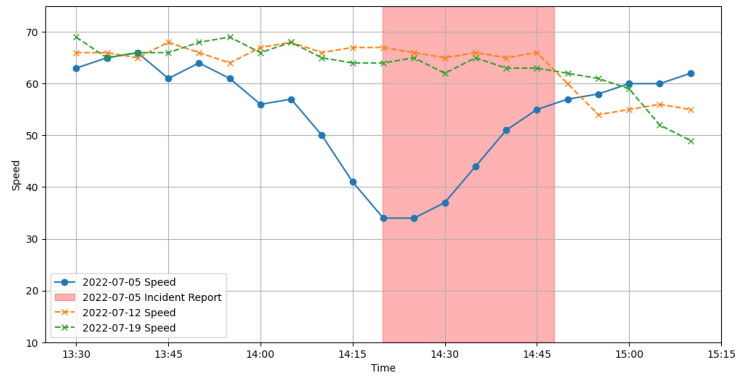
The main structure of this paper is as follows: Section 2 reviews existing AID research and identifies the research gaps. Section 3 introduces the data we used and the data processing methods. Section 4 describes our methodology in detail, including how to generate a new set of labels, address data imbalance issues, and employ



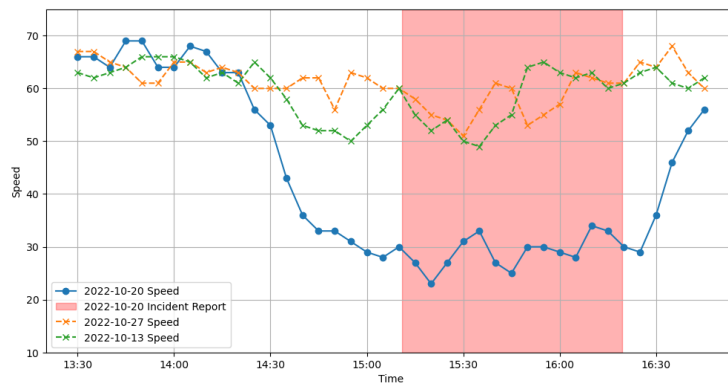
(a) 2022-06-28 Case



(b) 2022-07-01 Case

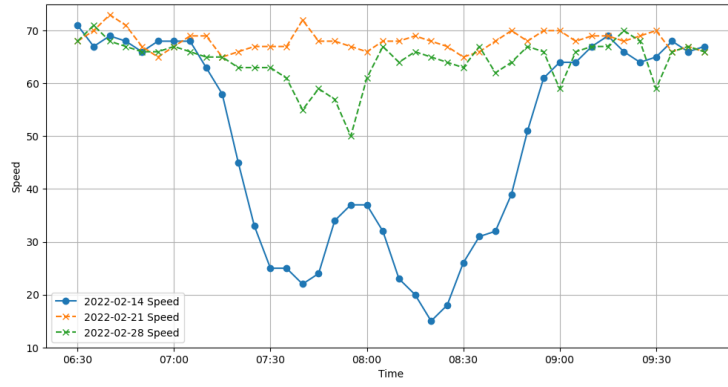


(c) 2022-07-05 Case

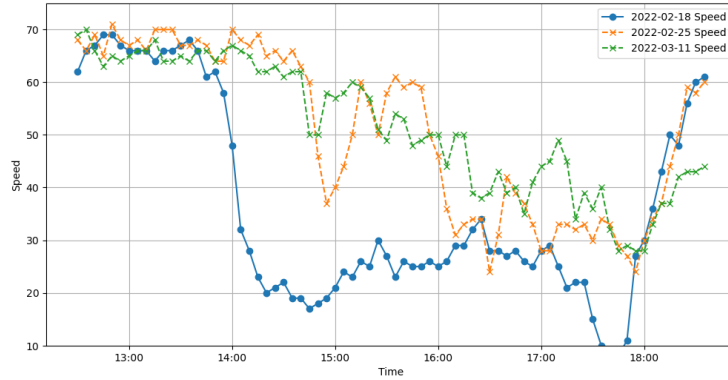


(d) 2022-10-20 Case

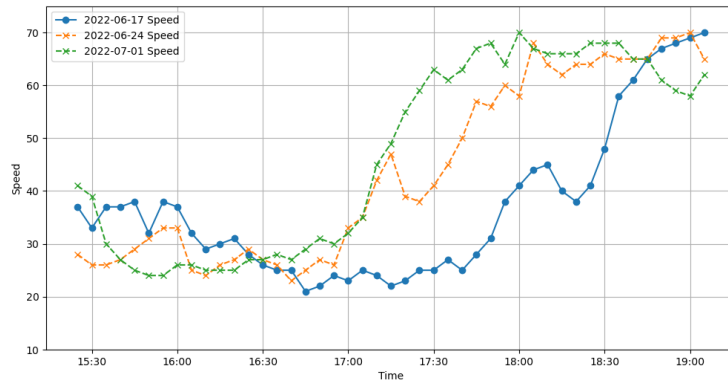
Figure 2: Time-varying speeds on a road segment: Waze incident reports were significantly delayed



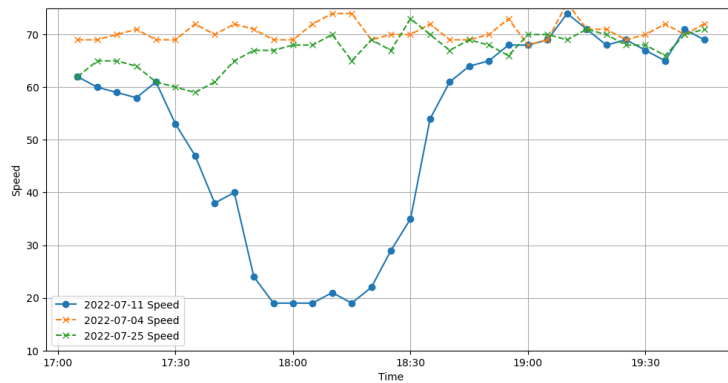
(a) 2022-02-14 Case



(b) 2022-02-18 Case



(c) 2022-06-17 Case



(d) 2022-07-11 Case

Figure 3: Time-varying speeds on a road segment: Incident reports were missing

design and training techniques to achieve data mining and effective model training. Section 5 demonstrates our framework’s data mining capabilities by comparing models trained with anomaly labels, followed by a comparison with incident reports. Section 6 provides a summary and outlines future research directions.

2 Literature Review

Research on Automatic Incident Detection (AID) began in the 1970s. Early traditional methods included statistical and competitive approaches. Statistical methods compare observed values with historical data, using statistical metrics such as standard normal derivative (SND) (Dudek et al., 1974) and inter-quartile distance (IQD) (Chakraborty et al., 2019) to measure differences. An alarm is triggered when an outlier is observed. However, without direct supervision by incident labels, outliers identified may not be anomalies, resulting in high false alarm rates. Another statistical approach measures the difference between predicted values and real observed values. Alarms are triggered when predictions significantly differ from observations. This is based on the assumption that traffic patterns can be accurately predicted under recurring conditions while not in non-recurring conditions. The forecasting models used are generally time-series, such as autoregressive integrated moving average (ARIMA) (S. A. Ahmed & Cook, 1982) and long short-term memory (LSTM) (Pan, 2022). This method performs well when observations are accurate, and the prediction model has low errors in recurring conditions. However, the same issue persists: these models lack supervised learning with anomaly labels, so outliers may not be anomalies. In fact, the observations are inherently noisy, and recurring conditions cannot ensure low prediction errors, especially during peak hours, resulting in poor detection performance.

Comparative methods collect traffic data such as flow, speed, and occupancy through detectors and compare them with past incident patterns. Alarms are triggered when the collected data matches a pre-defined incident pattern. Representative comparative methods include the California (Payne & Tignor, 1978), Manchester (Persaud & Hall, 1989), and Minnesota (Stephanedes & Chassiakos, 1993) algorithms. These methods are highly inspiring and have pioneered the analysis and extraction of incident characteristics. However, they largely remain at the level of manually summarizing incident characteristics, relying on pre-defined simple structures or patterns to determine whether to trigger an alert. The limited data mining capacity results in a high false alarm rate and mean time to detection.

Due to the richness and complexity of traffic data, researchers have begun to consider using artificial intelligence for data mining to detect incidents. Cheu and Ritchie (1995) used multi-layer feedforward neural networks (MLF) for incident detection, outperforming traditional methods on simulated data and small field data containing 9 incidents. To further validate feasibility on real-world data, Dia and Rose (1997) used data collected from Tullamarine Highway, Melbourne, demonstrating their feasibility on real datasets. Abdulhai and Ritchie (1999) optimized the model, proposing a Bayesian-based probabilistic neural network (BPNN), and trained the model using data from I-880, California, and I-35W, Minnesota. Jin et al. (2002) further optimized the model by proposing the constructive probabilistic neural network (CPNN) and conducted studies on the same experimental section of I-880. Given the strong performance of support vector machines (SVM) on binary classification problems, Yuan and Cheu (2003) proposed an SVM-based model and validated it on the datasets used by Jin et al. (2002) and Abdulhai and Ritchie (1999). To address the lack of incident samples, Lin et al. (2020) used generative adversarial networks (GANs) to generate more incident samples and use them combined with real incident samples to train an SVM classifier. Similarly, Li et al. (2022) used GANs on the same dataset as Lin et al. (2020) but replaced the SVM classifier with a temporal and spatially stacked autoencoder (TSSAE).

All the above research has utilized inductive-loop detectors, which can provide comprehensive data on traffic flow, occupancy, and speed. However, the reliance on loop detectors reduces the generalizability of the methods. For example, in the U.S., most highway segments do not have loop detectors installed. Even when installed, the density of the detectors is often insufficient to meet effective detection requirements. For instance, the loop detectors used by Lin et al. (2020); Yuan and Cheu (2003) and Li et al. (2022) are spaced about every 0.5 miles, which limits the applicability of these methods to only the road segments near the installed detectors. Other studies using traffic cameras (Chakraborty et al., 2018; Ki & Lee, 2007; Singh & Mohan, 2018) or high-precision GPS (Han et al., 2020; Sermons & Koppelman, 1996) also face similar issues. Very few studies have leveraged easily accessible data. Gu et al. (2016) and Zhang et al. (2018) utilized social media data for incident detection. However, social media is inherently a highly noisy form of manual reporting, facing issues such as irrelevance, delays, and missing, similar to traditional incident reports. In contrast, the speed data integrated from probe vehicles used by Sethi et al. (1995) provides an intuitive reflection of traffic conditions and is also easily accessible. Though Balke et al. (1996) pointed out that the limited penetration rate of probe vehicles leads to less prominent results, recent advancements in data collection methods have made the penetration rate of probe vehicle speed data increase. Cheu and Tay (2004) and Asakura et al. (2017) also explored the required penetration rate of probe vehicles to achieve efficient detection through simulation data. It should be acknowledged that probe vehicle speed data still faces high noise issues compared to detector data. As a result, related research remains quite limited. Recent progress using probe vehicle data in AID includes the method

proposed by [Chakraborty et al. \(2019\)](#), which combines bilateral filtering and total variation with statistical methods. However, there is still a lack of research utilizing other techniques, such as AI, which achieve better mining results on detector data than traditional statistical-based AID methods.

In addition to input data, another long-neglected issue is anomaly labels. Anomaly labels typically come from incident reports, but due to false reports and insignificant incidents, model training often fails to converge. Therefore, it has long been necessary to manually filter out real and impactful accidents. For example, [Dia and Rose \(1997\)](#) manually selected 60 out of 385 accidents, [Abdulhai and Ritchie \(1999\)](#) manually filtered and organized accident reports on I-880 California and I-35 Minnesota, and [Chakraborty et al. \(2019\)](#) combined manual selection with traffic cameras to filter incident reports. Subsequent researchers have widely used these datasets. Filtering and organizing incident reports requires significant manual effort, limiting the model’s generalizability. We also cannot utilize the existing abundance of incident reports to achieve model generalization. Furthermore, even after complex manual filtering, incident reports still have inherent issues, such as delays and missing, leading to a lack of relevant anomaly samples in the training data, which restricts the model’s performance. To address this issue, [Petty et al. \(1996\)](#) used driver manually calibrated data, but this is obviously impractical for most datasets. Current research still aligns prediction results with incident reports rather than anomalies. We need a model capable of achieving broader anomaly detection.

There are more approaches based on synthetic data, which we will not detail here due to challenges in real-world data collection. For more comprehensive literature reviews on automatic incident detection, please refer to [Parkany and Xie \(2005\)](#) and [ElSahly and Abdelfatah \(2022\)](#).

3 Data Preparation & Feature Engineering

We first discuss multiple data sources that are commonly available to use for early anomaly detection. Those data are most general in the sense they can be obtained to cover any geographic region and thus generally applicable to all locations. The data can be publicly available, or are offered by a number of data vendors with relatively mature technologies in the present market. In particular, we use incident reports, probe speed (segment level), and weather conditions for this study. Notably, all the information we use is gathered without the need to install additional detectors on the road network.

3.1 Incident Reports

Incident data can come from Waze and the State Departments of Transportation, which typically provide incident data feeds (real-time and historical). We select incident types that typically cause non-recurrent changes in traffic. Due to system discrepancies, the selected incident types vary slightly among various systems. The selected incidents mainly include accidents, hazardous weather, special events, and crashes. Those incident reports come with geographic locations and report time for each incident, which is translated to a binary indicator, $INC_i(t)$, denotes whether there is an incident report on link i at time t .

3.2 Speed Data

Raw Traffic Speed: In our experiments, speed data comes from INRIX, which calculates speeds through real-time monitoring of probe vehicles. Similar data can also be obtained from other sources, e.g., HERE, AirSage, TomTom, or telematics data. We use four types of INRIX speed data: 1-minute granularity speed for private vehicles, trucks, and all vehicles, as well as 5-minute granularity speed for all vehicles. To describe the speed on a link, we primarily refer to the 5-minute granularity speed for all vehicles, as it exhibits a lower noise level and provides a comprehensive measurement across different vehicle types.

$$v^i(t) := v^{i,5\text{-min}}(t) \tag{2}$$

where link i is in the segment defined by TMC (Traffic Message Channels), which is unified across multiple data vendors, $v^i(t)$ is the corresponding segment speed, and $v^{i,5\text{-min}}(t)$ is the 5-minute granularity speed for all vehicles of the segment. To impute missing 5-minute granularity speed data for all vehicles, we initially attempt to fill the gaps using the space mean speed from 1-minute granularity data for all vehicles, as described in Equation 3. If all the 1-minute data during that 5-minute interval are also missing, we infer that traffic flow is minimal so that no probe vehicles are present. In such cases, we use the free flow speed, defined as the 85th percentile speed, to fill in the missing data. This approach allows us to compile a complete dataset of 5-minute

speed data for all vehicles.

$$v^{i,5\text{-min}}(t) = \frac{\sum_{j=0}^4 \mathbb{I}(v^{i,1\text{-min}}(t-j\text{-min}) \neq \text{NaN})}{\sum_{j=0}^4 \{\mathbb{I}(v^{i,1\text{-min}}(t-j\text{-min}) \neq \text{NaN})/v^{i,1\text{-min}}(t-j\text{-min})\}} \quad (3)$$

The 5-minute speed data for trucks and private vehicles are also calculated from 1-minute granularity using Equation 3. To impute missing speed data for trucks and private vehicles, we initially calculate the ratio of non-missing speed data for trucks and private vehicles to that of all vehicles. We then multiply these ratios by the complete speed dataset for all vehicles to fill the gaps.

Slowdown Speed: We further perform feature engineering on the speed data. The slowdown speed as defined in Equation 4 is calculated,

$$SD^i(t) = \max\left(\frac{\sum_{j \in \tau^i} v^j(t)}{|\tau^i|} - v^i(t), 0\right) \quad (4)$$

where τ represents the set of upstream link segments within a certain distance range, and $|\cdot|$ denotes the number of elements in the set. Equation (4) means that for a target link segment i , its slowdown speed is the difference between a target link and the speed of all its upstream links. A large slowdown speed indicates the presence of a sudden back-of-sequence slowdown in the spatial domain (Yao & Qian, 2020), and has a high correlation with the occurrence of incidents according to the incident shock-wave theory (Wirasinghe, 1978).

Travel Time Index: We also calculate the travel time index (TTI) using the formula specified in Equation 5, where V^i denotes the speed distribution of segment i , and $\mathbb{P}_{0.85}(V^i)$ represents the 85th percentile speed. While the slowdown speed measures anomalies in the spatial dimension, the travel time index provides a comparison in the temporal dimension. Both the slowdown speed and travel time index calculations utilize the complete 5-minute granularity speed data for all vehicles.

$$TTI^i(t) = \max\left(\frac{\mathbb{P}_{0.85}(V^i)}{v^i(t)}, 1\right) \quad (5)$$

Seasonal Recurrent Speed: The travel time index measures speed anomalies in the temporal dimension but lacks seasonal and day-of-week patterns that the speed clearly exhibits. Therefore, we defined a seasonal recurrent speed (SRS) using Equation 6 to provide the model with a reference for recurrent speed under the current season and day-of-week. Equation 6 represents the mean speed on the same day of the week over the past three weeks, excluding any periods with incident reports. $INC_i(t) = 1$ when there is an incident report on link segment i at time t , and 0 otherwise.

$$SRS^i(t) = \frac{\sum_{j=1}^3 v^i(t-j*week) \mathbb{I}(INC^i(t-j*week) \neq 1)}{\sum_{j=1}^3 \mathbb{I}(INC^i(t-j*week) \neq 1)} \quad (6)$$

Sampling rate: Fixed location detectors (such as loop detectors, cameras, etc.) are typically needed to obtain flow data, which are generally unavailable in most roadway segments. Thus, we approximate the flow data with the data density provided along with TMC speed data. TMC data density depends on the number of probe vehicles when calculating segment speeds and is divided into three levels: A, B, and C, representing high, medium, and low probe vehicle numbers, respectively. This is obtained from INRIX data, but other data vendors provide similar measurements in terms of sampling rates or confidence levels. We will normalize the numbers by setting the data density for A, B, and C to 1, 2/3, and 1/3, respectively, and setting it to 0 when the probe speed data is missing.

3.3 Weather and Time Information

Weather: Weather data may be obtained from a few possible sources, e.g., open-meteo.com, NOAA NWS, metomatics.com, etc. We use seven features in a numerical format: temperature, humidity, hourly precipitation, hourly snowfall, hourly snow depth, hourly wind speed, and hourly wind direction.

Time: Our time features include month, week, day of the week, and time of the day. Since these features are all

periodic, we use sine and cosine functions to encode this information. The encoding formulas are as follows:

$$SIN(t) = \sin\left(\frac{2\pi t}{T}\right) \quad (7)$$

$$COS(t) = \cos\left(\frac{2\pi t}{T}\right) \quad (8)$$

where t is the time feature value, and T is the period of the feature (for example, the period for month is 12).

3.4 Data for experiments

As an experiment implemented in the later part of this paper, incident reports from two regions, Howard County, Maryland, and Cranberry Township, Pennsylvania, were collected for analysis. The data from Howard County spans 2022-2023, while data from Cranberry Township covers 2022-2024. Figure 4 shows the Traffic Message Channels (TMC) network (red lines) and the recorded incident locations (blue dots) for two regions.

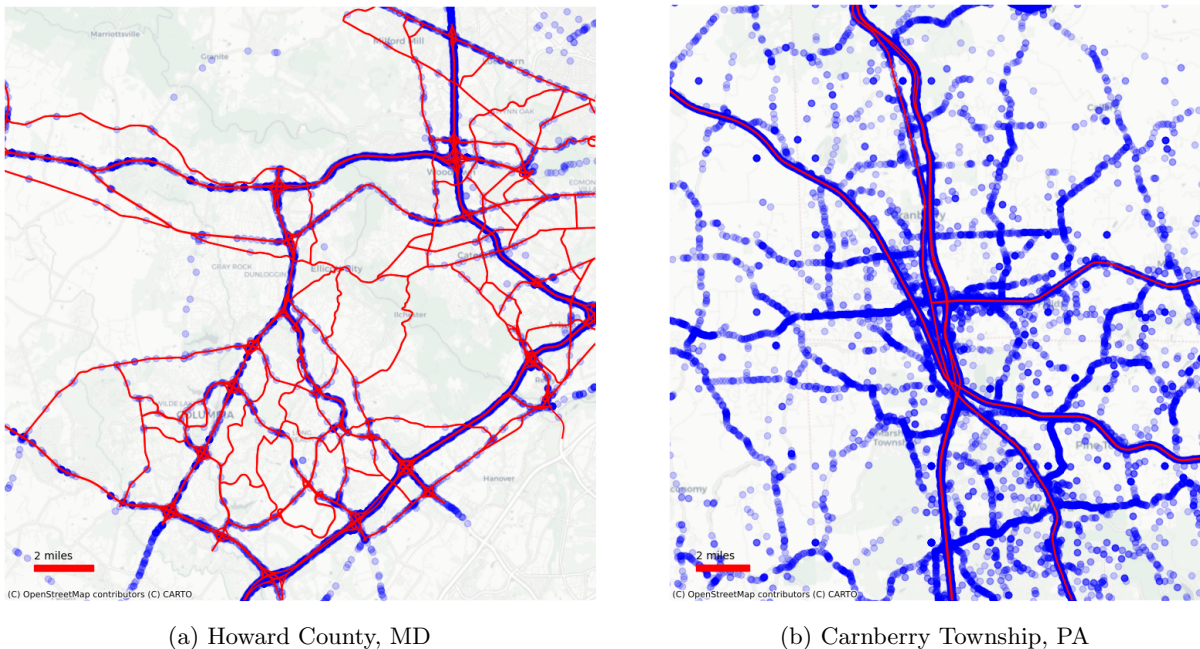


Figure 4: TMC Network and Incident Locations

4 Methodology

Our goal is to train an effective model in early anomaly detection/prediction. The model’s input consists of multi-source information over a past period, and the output is the anomaly status for a near future period. The incident reports are referenced for anomaly status labelling. To build an effective model, the following issues must be considered.

- **Rarity and randomness issues of the incident reports:** Regarding rarity, it leads to a severe imbalance between anomaly and normality data samples, which would hinder models from learning non-recurrent patterns. On the other hand, randomness may result in inconsistent data distributions between the training and validation/testing sets, posing challenges to model generalization.
- **Label quality issue:** Incident reports inherently have issues such as missing reports, delays, and false reports. Given that data points under anomalies are very scarce, directly using the presence of an incident report as an anomaly label can lead to substantial confusion between anomaly and non-anomaly data, making it difficult for the model to learn/train.

We propose a framework combining several strategies to address the above issues. The overall picture of the framework is depicted in Figure 5, where each dashed boxes corresponds to a strategy we used. The framework

first constructs a sub-graph for each link segment to establish the link-level anomaly prediction model. Then, by referencing and analyzing incident reports, we generate our anomaly labels (i.e., ground truth). With the inputs and labels in place, the data split module generates training, validation, and test data, ensuring no data leakage while maximizing the number of training samples. The model training section introduces the training techniques employed. In parallel with training, the model is calibrated to further enhance its performance. The details of each strategy will be introduced separately in this section.

4.1 Sub-Graph Construction

Constructing a sub-graph for each link segment is our first strategy to address the anomaly rarity issue. Specifically, we build a separate machine learning model for each segment to predict its anomaly status instead of using a single machine learning model to predict all link segments’ anomaly status. Though aiming for large-scale generalization, it is difficult to train a model to capture spatially or temporally variant incident probabilities and characteristics across different segments when anomaly data are scarce. Building separate models for each segment can reduce the complexity of the detection task.

Besides reducing the complexity of the task, the model complexity is also reduced by controlling the input dimensions, which has been theoretically proven to reduce the demand for extensive training samples (Hastie et al., 2009; Vapnik, 2013). The model’s input is limited to the traffic conditions within a certain range of upstream and downstream segments (which we refer to as a ”sub-graph”). This is based on the observation that an incident typically affects the traffic conditions of its upstream and downstream segments (Karim & Adeli, 2002), and this effect generally diminishes with distance. By inputting the sub-graph information, the input-output relevance and model complexity can be balanced.

4.2 Label Denoising by Prior Knowledge

Using incident reports directly as anomaly labels can introduce significant noise and hinder the convergence process. This is due to the inherent issues within incident reports, such as delays, missing, and inaccuracies. Additionally, not all incidents have a tangible impact on traffic conditions. For example, an incident on a multi-lane highway during off-peak hours might not affect speed or flow, thus resulting in an undetectable incident. This may not be of interest to traffic operators if there is no impact to mobility or safety for the time being. Consequently, using incident reports directly as labels can cause substantial confusion between anomaly and normality labels, diminishing their significance and learnability. To ensure the labels are meaningful and learnable, existing research typically uses a manual process to filter reported incidents; however, this introduces subjectivity and limits their scalability. Most importantly, manually selecting incident reports does not address the issue of missing reports, potentially causing unreported anomalies to be labeled as normal. Therefore, we propose a prior knowledge-based method for labeling anomalies. Besides filtering out insignificant or false reports, unreported incidents are also evaluated and labeled.

Given that traffic flow data often requires additional detectors and is not widely available, we use the slowdown speed described in Equation (4) as the prior knowledge to infer whether an incident report corresponds to a traffic anomaly. Theoretically, as explained in Section 3.2, a significant traffic incident of our interest should cause a significant slowdown speed. Table 1 empirically demonstrates the strong correlation between significant slowdown speeds and the occurrence of incidents. For instance, in the first row of Table 1, data from the Howard County reveals that only 1.27% of timestamps on the I-70 westbound study segment have incident reports. However, of those timestamps associated with the top 3% of highest slowdown speeds, 9.99% have incident reports, and over 60% of the entire incident reports fall within these top 3% slowdown speed timestamps. Other study segments in Table 1 also exhibit similar characteristics, revealing a high correlation between significant slowdown speeds and the occurrence of incidents.

Table 1: Correlation between Incident Report and Slowdown Speed

Study Segment Location	Region	Total Incident Reports (%)	Incident Reports in Top Slowdown Speeds (%)	Overlap with Incident Reports (%)
I-70W	Howard County, MD	1.27	9.99 (Top 3%)	60 (Top 3%)
I-70E	Howard County, MD	3.23	15.34 (Top 5%)	60 (Top 5%)
I-79S	Cranberry Township region, PA	3.81	13.40 (Top 5%)	65 (Top 5%)
I-79N	Cranberry Township region, PA	5.20	10.36 (Top 7%)	61 (Top 7%)

Our proposed prior knowledge-based denoising method is outlined in Algorithm 1. This method involves tuning a slowdown speed threshold for each link. If any point within the time frame of an incident report exceeds this threshold, the entire period is marked as an anomaly (Step 1). Additionally, any period during which the

Algorithm 1 Incident Label Denoising

Inputs: incident report binary matrix $\mathbf{INC}^i \in \mathbf{R}^{\text{number_of_days} \times \text{time_of_the_day}}$;
 slowdown speed matrix $\mathbf{SD}^i \in \mathbf{R}^{\text{number_of_days} \times \text{time_of_the_day}}$;
 removal percentage threshold θ_1 ;
 addition percentage threshold θ_2 ;
 minimum duration for a prolonged anomalies to be labeled θ_t

Outputs: anomaly label matrix $\mathbf{ANO}^i \in \mathbf{R}^{\text{number_of_days} \times \text{time_of_the_day}}$

Initialization: top $n\%$ slowdown speed is the indicator of anomalies

Step 0: Generate the abnormal slowdown speed matrix:
 obtain the abnormal slowdown speed threshold: $\theta_{\mathbf{SD}}^i = \text{Percentile}(\text{vec}(\mathbf{SD}^i), n)$
 compute the abnormal slowdown speed binary matrix: $\mathbf{ASD}_{(p,q)}^i = \mathbb{I}(\mathbf{SD}_{(p,q)}^i \geq \theta_{\mathbf{SD}}^i)$ for any element (p, q) in the matrix

Step 1: Remove insignificant incident reports:
 initialize the significant incident report matrix \mathbf{SIR}^i with zeros: $\mathbf{SIR}^i \leftarrow \mathbf{0}^{\text{number_of_days} \times \text{time_of_the_day}}$
 for $p = 0, 1, \dots, \text{number_of_days} - 1$ do
 for $q = 0, 1, \dots, \text{time_of_the_day} - 1$ do
 if $(q = 0 \text{ and } \mathbf{INC}_{(p,q)}^i = 1) \text{ or } (\mathbf{INC}_{(p,q-1)}^i = 0 \text{ and } \mathbf{INC}_{(p,q)}^i = 1)$ then \triangleright find the start of an incident report
 $r = 0$
 while $\mathbf{INC}_{(p,q+r)}^i = 1$ and $q + r \leq \text{time_of_the_day}$ do \triangleright check how long the incident report lasted
 $r \leftarrow r + 1$
 end while
 if $\text{SUM}(\mathbf{ASD}_{(p,q:r)}^i) \geq 1$ then \triangleright check if the incident report is significant
 set $\mathbf{SIR}_{(p,q:r)}^i = 1$
 end if
 end if
 end for
 end for

Step 2: Label prolonged significant anomalies:
 initialize the prolonged significant anomalies matrix \mathbf{PSA}^i with zeros: $\mathbf{PSA}^i \leftarrow \mathbf{0}^{\text{number_of_days} \times \text{time_of_the_day}}$
 for $p = 0, 1, \dots, \text{number_of_days} - 1$ do
 for $q = 0, 1, \dots, \text{time_of_the_day} - 1$ do
 if $(q = 0 \text{ and } \mathbf{ASD}_{(p,q)}^i = 1) \text{ or } (\mathbf{ASD}_{(p,q-1)}^i = 0 \text{ and } \mathbf{ASD}_{(p,q)}^i = 1)$ then \triangleright find the start of an anomaly
 $r = 0$
 while $\mathbf{ASD}_{(p,q+r)}^i = 1$ and $q + r \leq \text{time_of_the_day}$ do \triangleright check how long the anomaly lasted
 $r \leftarrow r + 1$
 end while
 if $r \geq \theta_t$ then \triangleright check if the anomaly is prolonged
 set $\mathbf{PSA}_{(p,q:r)}^i = 1$
 end if
 end if
 end for
 end for

Step 3: Check the removal and addition percentage threshold:
 compute the removal percentage $\text{rm}\% = 1 - (\text{SUM}(\mathbf{SIR}^i) / \text{SUM}(\mathbf{INC}^i))$
 determine which labels are newly added $\mathbf{ADD}^i = \text{ReLU}(\mathbf{ASD}^i - \mathbf{INC}^i, 0) = \text{ReLU}(\mathbf{ASD}^i - \mathbf{SIR}^i, 0)$
 compute the addition percentage $\text{add}\% = \text{SUM}(\mathbf{ADD}^i) / \text{SUM}(\mathbf{INC}^i)$
 if $\text{rm}\% > \theta_1$ and $\text{add}\% \leq \theta_2$ then
 $n \leftarrow n + \alpha$
 Go back to **Step 0**
 else if $\text{rm}\% \leq \theta_1$ and $\text{add}\% > \theta_2$ then
 $n \leftarrow n - \alpha$
 Go back to **Step 0**
 else if $\text{rm}\% \leq \theta_1$ and $\text{add}\% \leq \theta_2$ then
 Go to **Step 4**
 else
 the settings of θ_1 and θ_2 are unreasonable, terminate the algorithm and reinitialize
 end if

Step 4: Generate anomaly labels:
 combine significant incident report and newly added labels by $\mathbf{ANO}^i = \mathbf{SIR}^i + \mathbf{ADD}^i$
 output \mathbf{ANO}^i

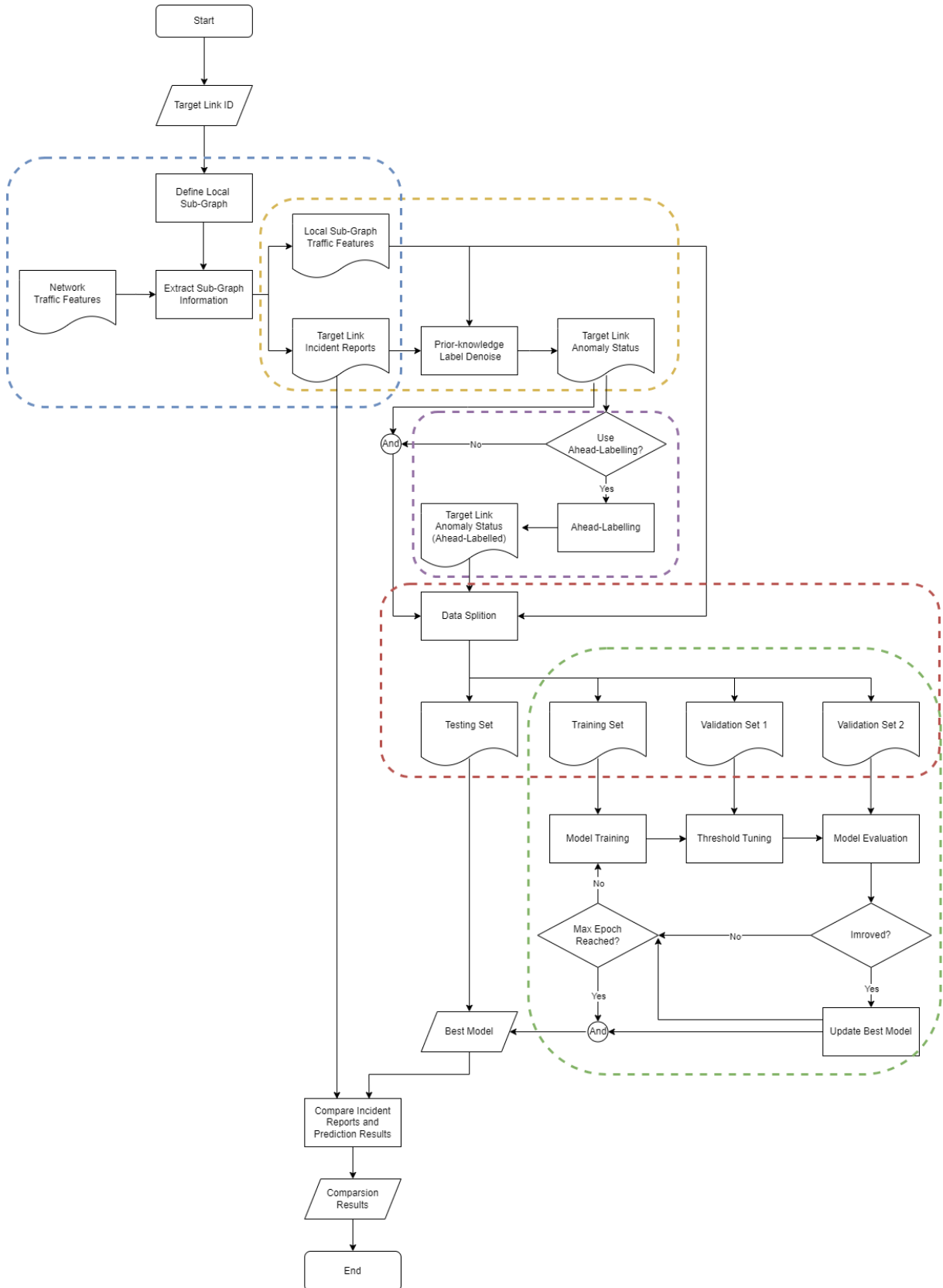


Figure 5: High-level System Diagram

slowdown speed consistently exceeds this threshold is also marked as an anomaly (Step 2). Furthermore, we control the ratio of removal and addition anomaly labels by setting θ_1 and θ_2 (Step 3). It is important to note that the denoising process does not generate a new set of labels solely based on abnormal slowdown speed. The

model is not trained to detect abnormal slowdown speeds. According to our rules, if an abnormal slowdown speed is detected at any timestamp within an incident report, all timestamps corresponding to that report will be marked as anomalies. This means not all points marked as anomalies necessarily exhibit abnormal slowdown speeds. Conversely, not every timestamp with abnormal slowdown speed will be labeled as an anomaly. The criteria for adding missing reports require that an abnormal slowdown speed must persist for at least θ_t steps to be labeled as an anomaly. In summary, abnormal slowdown speed is neither a sufficient nor a necessary condition for anomaly labeling. The default thresholds we set for θ_1 , θ_2 , and θ_t are 0.6, 1.0, and 3 (15 min as the prediction interval is 5 min), respectively. These values may be subject to slight adjustments based on the data collected.

4.3 Ahead Labeling

The algorithm 1 mainly extracts common features from incident reports. However, as shown in Figure 2, incident reports often lack the early stage of incidents. While algorithm 1 can label some missing or delayed reports, they do not address the inherent delay issue in the reporting process. Therefore, we label anomalies starting from a few time steps prior to the reported incident/anomaly time to supplement the lack of early characteristics in the anomaly samples. For example, an anomaly from 7:30 a.m. to 8:30 a.m. can be ahead-labeled by 15 minutes to become from 7:15 a.m. to 8:30 a.m. The algorithm is shown in Algorithm 2. The setting of θ_{ahead} balances the inclusion of early features and false anomalies. The larger the θ_{ahead} , the more early incident features are included, but it also increases the likelihood of normal samples being labeled as anomalies. Practically, this would need to be tuned for each road segment or to the traffic operator’s preference. In our experiment, we use 3 as the default value of θ_{ahead} , which is 15 minutes given the prediction interval is 15 minutes.

Algorithm 2 Anomaly Ahead Labeling

Inputs: anomaly label matrix $\mathbf{ANO}^i \in \mathbf{R}^{number_of_days \times time_of_the_day}$
ahead label duration θ_{ahead}
Outputs: ahead-labeled anomaly label matrix $\mathbf{AAN}^i \in \mathbf{R}^{number_of_days \times time_of_the_day}$
initialize the ahead-labeled anomaly label matrix \mathbf{AAN}^i with the anomaly label matrix $\mathbf{AAN}^i \leftarrow \mathbf{ANO}^i$
for $p = 0, 1, \dots, number_of_days - 1$ **do**
 for $q = 1, \dots, \theta_{ahead} - 1$ **do**
 if $\mathbf{ANO}_{(p,q)}^i = 1$ **then** ▷ find the start of an anomaly
 $\mathbf{AAN}_{(p,:q)}^i = 1$
 end if
 end for
 for $q = \theta_{ahead} - 1, \dots, time_of_the_day - 1$ **do** ▷ find the start of an anomaly
 if $\mathbf{ANO}_{(p,q)}^i = 1$ and $\mathbf{ANO}_{(p,q-1)}^i = 0$ **then**
 $\mathbf{AAN}_{(p,q-\theta_{ahead}:q)}^i = 1$
 end if
 end for
end for
output \mathbf{AAN}^i

4.4 Multi-step Prediction & Data Splitting

Conventional AID typically formulates its task as a single-step prediction, i.e., determining whether the road segment is currently in incident status. To promote early detection, in our model, we formulate an anomaly detection/prediction task as a multi-step prediction, predicting the anomaly status in the next few steps. In this case, if the model captures the early incident features, even if it may not cause anomaly in this step but a few steps later, the model will still be able to give an alert.

Multi-step anomaly prediction/detection on past traffic conditions can be formulated as a sequence-to-sequence prediction task. To mitigate the issue of limited samples, we use a sliding window to increase sample numbers by partitioning the dataset into multiple subsections. As illustrated in Figure 6, suppose our study period is from 6 AM to 9 PM, and we use past 1 hour’s data to predict the anomaly status for the next half hour, with predictions made every five minutes. Then, the first sample of the day is using data collected between 6:00 AM-6:55 AM to predict the anomaly status between 7:00 AM-7:25 AM; the second sample is using data collected between 6:05 AM-7:00 AM to predict the anomaly status between 7:05 AM-7:30 AM, and so on. Using a sliding window can increase the number of training samples to mitigate the limited data issues.

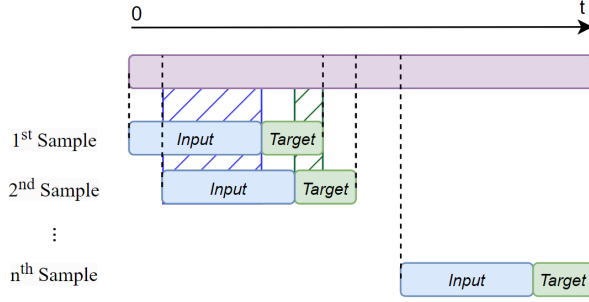


Figure 6: Sliding Window and Train-Test Contamination

However, it is crucial to note that applying the sliding window must strictly occur after splitting the dataset. That is, we need to first divide the data into training, validation, and test sets and then apply the sliding window within each dataset. If the sliding window is applied to the entire dataset first and then randomly shuffled to create the training and test sets, it will result in data leakage, also known as train-test contamination. This occurs because information from the test set can inadvertently be mixed into the training set. As shown in Figure 6, the 1st and the 2nd samples, although not identical, have a high degree of overlap in both inputs and targets (see the hatch part). If they are assigned to the training and test sets respectively, even if the model overfits the 1st sample, testing using the 2nd sample may still produce good results due to its high similarity to the 1st sample, giving a false evaluation of model performance. We further verified by experiment that a model trained with train-test contamination performs poorly on a new dataset without data contamination.

4.5 Model Training

This framework is applicable to various classical deep-learning models based on encoder-decoder structures, including Seq2Seq (Sutskever et al., 2014), Seq2Seq models with attention mechanisms (Bahdanau et al., 2014), Transformer (Vaswani et al., 2017), and GraphTrans (Wu et al., 2021). As mentioned in Section 4.1, the traffic status of the sub-graph over the past period is fed into the encoder, and then the decoder outputs the anomaly status of the target link for the future period in an auto-regressive manner.

Weighted binary cross-entropy (WBCE), as shown in Eq.(9), is used as the loss function for model training, where w_{ano} denotes the additional weight for anomaly samples, \hat{y}_i denotes the predicted value, and y_i denotes the label value (1 for anomaly sample and 0 for normality sample).

$$L = -\frac{1}{N} \sum_{i=1}^N (w_{ano} y_i \log(\hat{y}_i) + (1 - y_i) \log(1 - \hat{y}_i)) \quad (9)$$

When $w_{ano} = 1$, Eq.(9) is the binary cross-entropy (BCE), which is commonly used for binary classification training due to its differentiability. The purpose of weighting is to overcome the imbalance in datasets caused by the scarcity of anomaly samples. Without weighting, the predominance of normality samples would bias the model to consistently output zero. For the setting of w_{ano} , the default practice is to divide the number of samples whose label are 0 (normality samples) by the number of samples whose label are 1 (anomaly samples). Further adjustment is a trade-off between recall and precision (definitions refer to Figure 7). Increasing the weight helps to improve recall, while decreasing it helps improve precision.

During model training, we employ the teacher forcing technique (Williams & Zipser, 1989) in the auto-regressive decoder to accelerate and enhance convergence. Teacher forcing is a widely adopted strategy in contemporary natural language processing (NLP) model training. This method involves substituting the decoder’s prior outputs with actual labels during subsequent computations in the training phase.

4.6 Threshold Adaptation

The trained model outputs a number between 0 and 1, which can be interpreted as a probability of an anomaly; however, determining when to trigger an alert still requires a threshold. The practice of using 0.5 as a threshold in a balanced dataset assumes that the model can perfectly output values close to 0 and 1. However, due to the setting of w_{ano} and the model’s inability to converge perfectly, the 0.5 threshold lacks theoretical basis and may perform poorly. Therefore, it is necessary to tune an appropriate threshold for best model selection and development purposes.

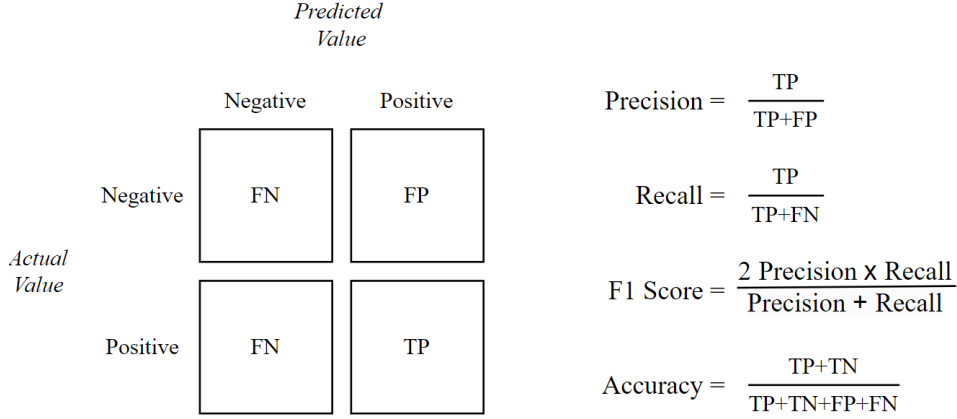


Figure 7: Recall, Precision, and F1 score

To prevent overfitting on the training data, threshold-tuning and model selection is performed on a validation set. Considering that incidents occur randomly, the distribution of anomaly samples in the validation set may differ from that in the training set. Therefore, we use the F1 score for model selection. The validation set is divided into two parts. The validation set 1 is used to find the threshold that maximizes the F1 score in validation set 1. With the tuned threshold, we can select the best model by optimizing the F1 score in validation set 2. Validation set 2 serves to simulate the test set. In this way, the model is selected based on a threshold that adapts to the model output, avoiding the issue of discarding well-performing models due to a fixed threshold.

Similar to the setting of w_{ano} , depending on emphasis on precision and recall, other F-scores can be used. Here, β is the hyper parameter, meaning that recall is β time more important than precision.

$$F_{\beta} = (1 + \beta^2) \cdot \frac{\text{Precision} \times \text{Recall}}{(\beta^2 \cdot \text{Precision}) + \text{Recall}} \quad (10)$$

5 Results and Discussion

This section is divided into two parts: the results of early anomaly detection (with possible prediction) and incident report comparison. In the early anomaly detection part, we use the generated anomaly label (ground truth) as a reference to assess our model’s ability to detect or predict significant anomalies in advance. In the incident report comparison part, we will compare our prediction results to raw incident reports (with inaccurate, insignificant, missing, or delayed reports).

5.1 Early Anomaly Detection/Prediction

Our experiments were conducted on the two road networks introduced in Section 3. We divided our training, testing, and validation sets in a 7:2:1 ratio in chronological order. We chose the periods that are relatively more challenging to predict: Predictions were made on weekdays, from 6:00 a.m. to 8:30 p.m., forecasting the anomaly status for the next half hour.

We first show the relationship between recall, precision, F1 score, and accuracy of the model as the threshold changes. Taking the Howard County I-70 segment as an example, Figure 8 shows the recall, precision, and F1 score for predicting anomaly status 5 minutes, 15 minutes, and 25 minutes ahead. The left side shows the results of the validation set, and the right side shows the results of the test set. From the figures, it can be observed that the model’s performance on the validation set is almost identical to that on the test set. As the prediction period increases, the best F1 score gradually decreases. As the threshold increases, recall increases while precision decreases. Selecting an appropriate threshold allows us to achieve high accuracy and a high F1 score. The range for this threshold is approximately between 0.5 and 0.7. Figure 9 shows the results trained with 15-minute ahead labeling. Similarly, as the prediction period increases, the best F1 score decreases. As the threshold increases, recall improves while precision drops. Selecting a threshold between 0.4 and 0.6 can balance recall and precision, ensuring high accuracy. It is worth noting that the ground truth differs between the cases with and without ahead labeling, so directly comparing these evaluation metrics between Figure 8 and Figure 9 lacks significance.

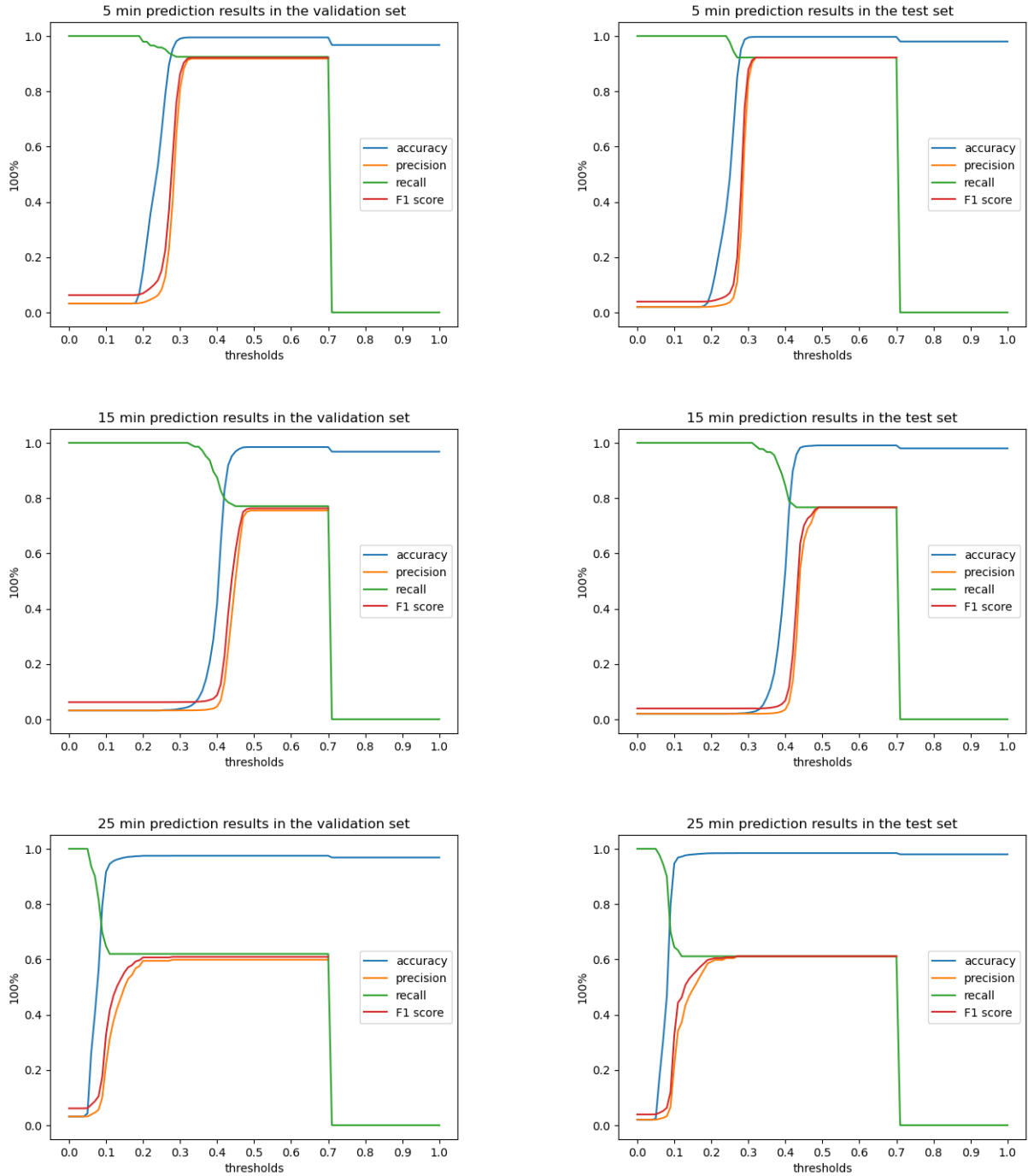


Figure 8: Recall, Precision, F1 score, Accuracy Plot (Without Ahead Labelling)

To validate the scalability of our method, we conducted experiments on 10 highway segments across two road networks. Tables 2 and 3 show the results. To avoid the interference of θ_{ahead} settings affecting the quality of the labels and thus reducing the persuasiveness of the results, Tables 2 and 3 use results without the ahead label. The effect of the ahead label will be discussed in the next chapter.

All the baseline models have been well-tuned and trained. The abbreviations represent the following:

- **RF**, Random Forest. Tree-based models are considered to perform well on imbalanced data and time-series predictions. We trained six RF models for prediction models ranging from 5 minutes to 30 minutes.
- **SVM**, Support Vector Machine, trained using the Radial Basis Function (RBF) kernel. Due to the impracticality of the computation time required for upsampling, we used downsampling for training. We trained six SVM models for prediction models ranging from 5 minutes to 30 minutes, in 5-min time

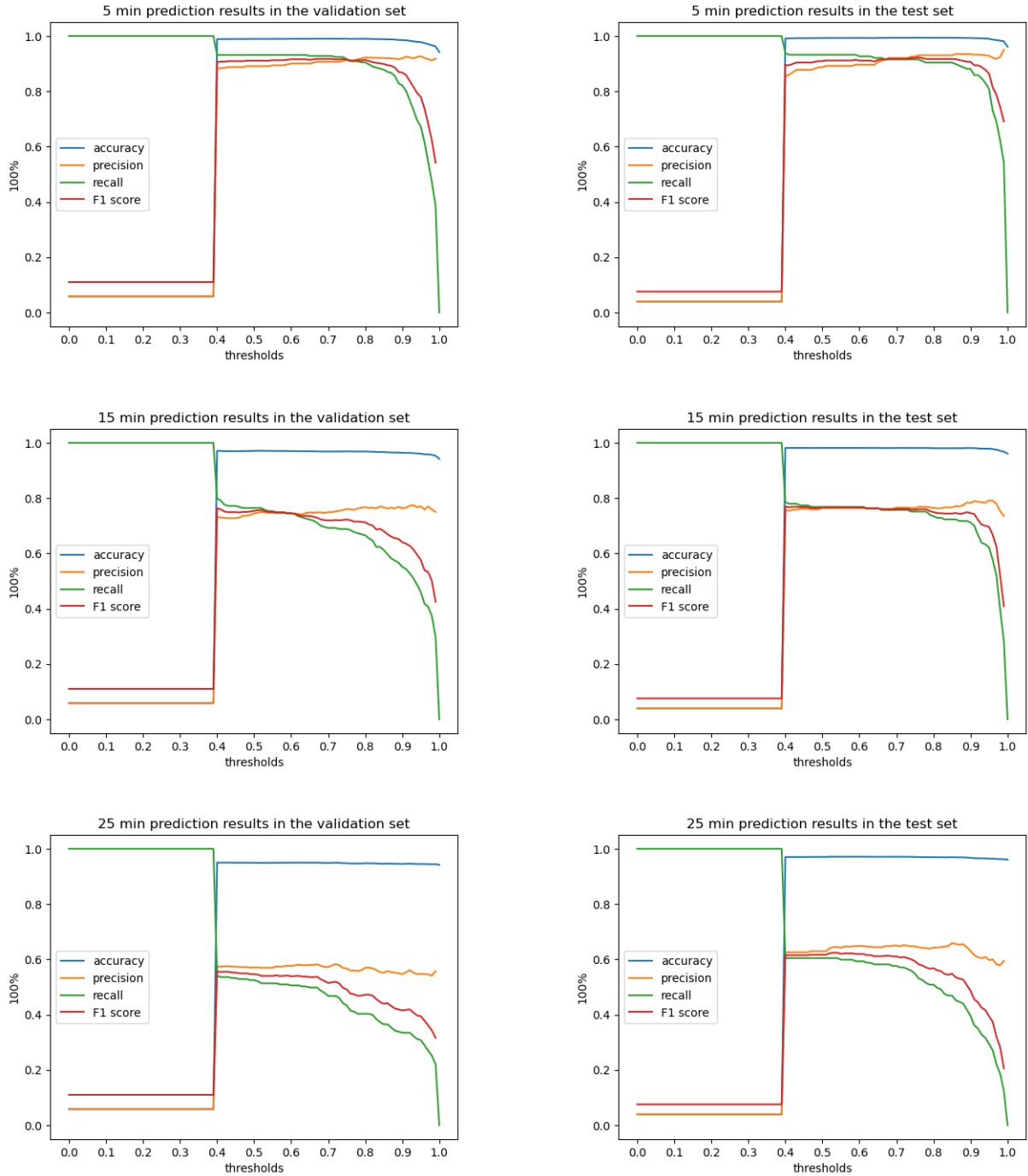


Figure 9: Recall, Precision, F1 score, Accuracy Plot (With Ahead Labelling)

increments.

- **GAN**, Generative Adversarial Net (Goodfellow et al., 2014). We first used GAN to learn the characteristics of anomaly samples and generate more anomaly samples to overcome the sample rareness issue. SVM is then used for classification. Similar to SVM, we need to build six models.
- **LightGBM**, Light Gradient Boosting Machine (G. Ke et al., 2017). LightGBM is an efficient gradient boosting framework that uses tree-based learning algorithms. It is designed to be distributed and efficient, capable of handling large-scale data. For prediction models ranging from 5 minutes to 30 minutes, we trained six LightGBM models.
- **Trans**: Our model trained with Transformer (Vaswani et al., 2017).
- **GTrans**: Our model trained with GraphTrans (Wu et al., 2021).

From the two tables, it is evident that the choice of model significantly impacts prediction performance. Overall,

the results of Trans and GTrans used in our method generally rank first and second but show slight differences. GTrans performs slightly better on most segments, likely due to its ability to capture topological structures. GAN and LightGBM stand out among the other baseline models. Although both use SVM as the classifier, GAN’s overall performance is superior to SVM, demonstrating the significance of generating additional anomaly samples using GAN proposed by Lin et al. (2020). Compared to RF, LightGBM performs better, which aligns with LightGBM’s suitability for handling high-dimensional data. Notably, in the results for I-79 and I-76 in Cranberry, our model is outperformed by GAN in predicting anomalies at 20, 25, and 30 minutes. We believe this is because we use a shared decoder for all six predictions, whereas GAN trains six separate models. It can be observed that our model’s prediction performance at 5, 10, and 15 minutes is significantly better than GAN’s, likely because the shared decoder primarily learns to predict shorter time intervals rather than longer ones.

5.2 Incident Report Comparison

In this section, we will compare our model’s prediction results with incident reports and conventional AID methods. Both incident reports and conventional AID methods use a single value to describe whether a road is in an incident state at a given time step. However, to achieve earlier detection and provide operators with a reference for road conditions over a future period (rather than just a single point in time), we employed multi-step predictions, forecasting road conditions for the next half hour. To compare multi-prediction with a single value, we adopted a conservative strategy by taking the minimum value among these six predictions as the measurement standard. If this minimum value exceeds the threshold, an alert is triggered; otherwise, no alert is triggered.

5.2.1 Detection Examples

Using I-70 as an example, our prediction process during the evening period on 2023-01-11 is detailed in Appendix A. In this example, we use our model trained with the ahead labelling strategy. In Appendix A, the red dashed line at 0.56 represents the adaptive threshold the validation set generated. At 17:15, our model’s predictions for the next six time steps are all below the threshold, so no alert is triggered (the blue line is used to indicate no alert). However, at 17:25, the minimum value exceeds the threshold, triggering an alert (the red line is used to indicate an alert). This alert ends at 17:45, as the minimum predicted value falls below the threshold at that time. The black text in Appendix A represents the current speed at the predicted time, while the red shading indicates the report time. From this, it can be observed that our model triggered an alert earlier than the incident report and even before the speed significantly dropped.

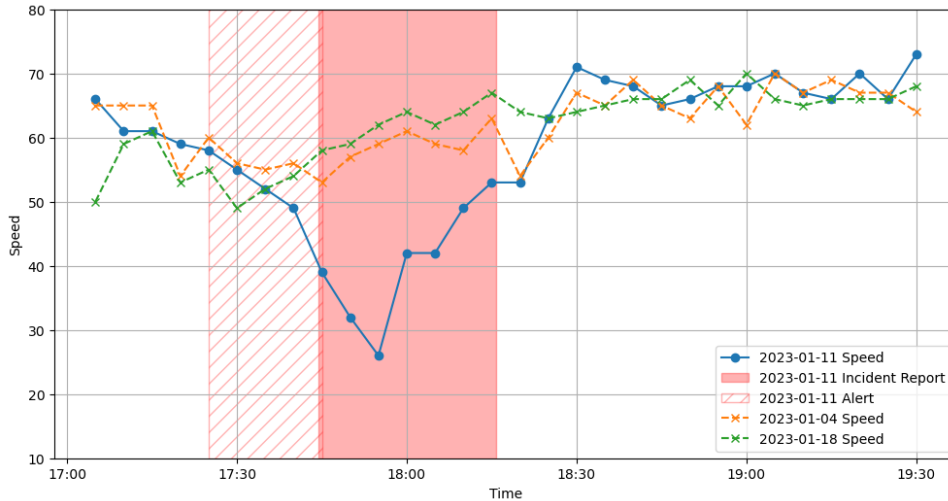


Figure 10: Speed, Alert, and Incident Report on 2023-01-11

To facilitate observation, we compiled the alert, incident report, and speed reference for the case in Appendix A in Figure 10. By analyzing the speed on that day and comparing it with the speed on nearby days without incident reports (same day of the week, same time of day), we observed that at 17:25, although the speed of the target segment did not change significantly and seemed to exhibit a recurrent pattern, our model still triggered the alert. Figure 11 shows the possible reasons for our model’s early detection. While it is difficult to observe from the target segment alone, the speeds upstream and downstream had already exhibited clear incident

Location		Metrics	Model	Time					
County	Road			5min	10min	15min	20min	25min	30min
Howard, MD	I-70E	Recall	RF	0.63	0.52	0.38	0.26	0.18	0.08
			SVM	0.89	0.87	0.86	0.84	0.80	0.75
			GAN	0.87	0.86	0.83	0.78	0.73	0.69
			LightGBM	0.79	0.76	0.70	0.58	0.53	0.46
			Trans	0.91	0.83	0.74	0.67	0.59	0.52
			G-Trans	0.91	0.83	0.74	0.67	0.62	0.52
		Precision	RF	0.79	0.73	0.68	0.62	0.54	0.42
			SVM	0.38	0.34	0.29	0.26	0.21	0.19
			GAN	0.47	0.43	0.40	0.36	0.31	0.28
			LightGBM	0.84	0.75	0.68	0.70	0.6	0.55
			Trans	0.91	0.77	0.63	0.49	0.38	0.33
			G-Trans	0.91	0.83	0.74	0.67	0.60	0.52
		F1 Score	RF	0.70	0.61	0.48	0.37	0.28	0.13
			SVM	0.54	0.49	0.43	0.40	0.34	0.30
			GAN	0.61	0.57	0.54	0.49	0.43	0.39
			LightGBM	0.81	0.75	0.68 [†]	0.64 [†]	0.56 [†]	0.50 [†]
			Trans	0.91*	0.80 [†]	0.68 [†]	0.57	0.47	0.41
			G-Trans	0.91*	0.83*	0.74*	0.67*	0.61*	0.52*
Howard, MD	I-70W	Recall	RF	0.52	0.35	0.22	0.07	0.01	-
			SVM	0.94	0.84	0.80	0.70	0.61	0.52
			GAN	0.86	0.75	0.67	0.59	0.52	0.45
			LightGBM	0.84	0.84	0.77	0.68	0.59	0.58
			Trans	0.90	0.77	0.67	0.58	0.51	0.43
			G-Trans	0.90	0.80	0.68	0.49	0.41	0.38
		Precision	RF	0.77	0.65	0.60	0.36	0.14	-
			SVM	0.38	0.28	0.23	0.19	0.17	0.13
			GAN	0.60	0.46	0.36	0.31	0.24	0.20
			LightGBM	0.68	0.59	0.40	0.37	0.31	0.21
			Trans	0.90	0.80	0.71	0.62	0.54	0.46
			G-Trans	0.81	0.79	0.68	0.60	0.51	0.48
		F1 Score	RF	0.62	0.45	0.32	0.12	0.03	-
			SVM	0.54	0.42	0.36	0.30	0.27	0.21
			GAN	0.71	0.57	0.46	0.40	0.33	0.28
			LightGBM	0.75	0.69	0.53	0.48	0.41	0.30
			Trans	0.90*	0.79*	0.69*	0.60*	0.52*	0.45*
			G-Trans	0.85 [†]	0.79*	0.68 [†]	0.54 [†]	0.45 [†]	0.42 [†]
Howard, MD	US-40E	Recall	RF	0.31	0.21	0.13	0.10	0.06	0.05
			SVM	0.81	0.80	0.82	0.75	0.74	0.71
			GAN	0.57	0.49	0.43	0.37	0.33	0.30
			LightGBM	0.61	0.50	0.42	0.39	0.31	0.30
			Trans	0.85	0.70	0.57	0.50	0.45	0.40
			G-Trans	0.85	0.70	0.57	0.50	0.45	0.40
		Precision	RF	0.84	0.77	0.81	0.87	0.75	0.69
			SVM	0.17	0.11	0.09	0.10	0.08	0.07
			GAN	0.66	0.61	0.57	0.61	0.53	0.55
			LightGBM	0.55	0.46	0.38	0.36	0.41	0.40
			Trans	0.85	0.71	0.58	0.51	0.45	0.41
			G-Trans	0.85	0.71	0.58	0.51	0.45	0.41
		F1 Score	RF	0.45	0.33	0.23	0.19	0.12	0.09
			SVM	0.28	0.19	0.16	0.17	0.15	0.12
			GAN	0.61	0.55	0.49	0.46	0.41	0.39
			LightGBM	0.58	0.48	0.40	0.37	0.36	0.34
			Trans	0.85*	0.71*	0.57*	0.50*	0.45*	0.40*
			G-Trans	0.84 [†]	0.71*	0.57*	0.50*	0.45*	0.40*
Howard, MD	US-40W	Recall	RF	0.43	0.35	0.20	0.17	0.07	0.05
			SVM	0.81	0.76	0.74	0.73	0.70	0.68
			GAN	0.62	0.58	0.52	0.50	0.47	0.45
			LightGBM	0.60	0.55	0.55	0.37	0.28	0.26
			Trans	0.86	0.73	0.60	0.51	0.45	0.42
			G-Trans	0.86	0.73	0.60	0.51	0.45	0.42
		Precision	RF	0.71	0.56	0.38	0.35	0.22	0.23
			SVM	0.26	0.19	0.14	0.11	0.10	0.16
			GAN	0.38	0.31	0.25	0.21	0.16	0.12
			LightGBM	0.68	0.40	0.33	0.29	0.33	0.31
			Trans	0.82	0.73	0.61	0.53	0.47	0.44
			G-Trans	0.86	0.74	0.61	0.53	0.47	0.44
		F1 Score	RF	0.53	0.43	0.26	0.22	0.10	0.08
			SVM	0.40	0.30	0.23	0.19	0.17	0.09
			GAN	0.47	0.40	0.33	0.30	0.24	0.19
			LightGBM	0.64	0.46	0.41	0.33	0.30	0.28
			Trans	0.84 [†]	0.73*	0.60*	0.52*	0.46*	0.43*
			G-Trans	0.86*	0.73*	0.60*	0.52*	0.46*	0.43*
Howard, MD	I-695A	Recall	RF	0.07	0.01	0.01	0.01	-	-
			SVM	0.91	0.85	0.83	0.78	0.74	0.66
			GAN	0.59	0.83	0.75	0.70	0.66	0.61
			LightGBM	0.75	0.63	0.48	0.42	0.32	0.60
			Trans	0.87	0.75	0.65	0.60	0.55	0.50
			G-Trans	0.87	0.74	0.65	0.59	0.55	0.50
		Precision	RF	0.89	1.00	1.00	1.00	-	-
			SVM	0.26	0.23	0.21	0.19	0.18	0.16
			GAN	0.44	0.40	0.38	0.38	0.37	0.36
			LightGBM	0.77	0.75	0.49	0.51	0.59	0.36
			Trans	0.87	0.76	0.66	0.62	0.56	0.51
			G-Trans	0.88	0.76	0.67	0.61	0.57	0.52
		F1 Score	RF	0.13	0.02	0.02	0.02	-	-
			SVM	0.40	0.36	0.34	0.31	0.29	0.26
			GAN	0.59	0.54	0.50	0.49	0.48	0.45
			LightGBM	0.76	0.68	0.49	0.46	0.41	0.45
			Trans	0.87 [†]	0.76*	0.66*	0.61*	0.55 [†]	0.51*
			G-Trans	0.88*	0.75 [†]	0.66*	0.60 [†]	0.56*	0.51*

Table 2: Howard County Anomaly Detection/Prediction Results

Location		Metrics	Model	Time					
County	Road			5min	10min	15min	20min	25min	30min
Cranberry, PA	I-79S	Recall	RF	0.36	0.26	0.24	0.19	0.20	0.18
			SVM	0.62	0.51	0.43	0.38	0.45	0.37
			GAN	0.43	0.36	0.31	0.29	0.27	0.25
			LightGBM	0.37	0.37	0.28	0.21	0.22	0.19
			Trans	0.80	0.64	0.35	0.28	0.26	0.27
			G-Trans	0.81	0.64	0.46	0.37	0.32	0.32
		Precision	RF	0.76	0.67	0.65	0.52	0.53	0.52
			SVM	0.08	0.07	0.07	0.07	0.07	0.06
			GAN	0.39	0.44	0.44	0.42	0.41	0.44
			LightGBM	0.38	0.29	0.31	0.36	0.27	0.26
			Trans	0.79	0.62	0.46	0.39	0.36	0.38
			G-Trans	0.78	0.63	0.46	0.37	0.32	0.32
		F1 Score	RF	0.44	0.38	0.35	0.28	0.29	0.27
			SVM	0.15	0.13	0.11	0.11	0.12	0.10
			GAN	0.41	0.40	0.36	0.35 [†]	0.32*	0.32*
			LightGBM	0.38	0.33	0.30	0.27	0.24	0.22
			Trans	0.79 [†]	0.58 [†]	0.40 [†]	0.32	0.30	0.31
			G-Trans	0.80*	0.63*	0.46*	0.37*	0.32*	0.32*
Cranberry, PA	I-79N	Recall	RF	0.19	0.11	0.10	0.09	0.09	0.11
			SVM	0.71	0.62	0.59	0.58	0.61	0.57
			GAN	0.52	0.39	0.33	0.29	0.27	0.23
			LightGBM	0.36	0.31	0.38	0.37	0.22	0.25
			Trans	0.77	0.49	0.32	0.23	0.16	0.13
			G-Trans	0.78	0.58	0.38	0.28	0.22	0.18
		Precision	RF	0.44	0.31	0.28	0.29	0.32	0.38
			SVM	0.15	0.15	0.13	0.13	0.12	0.11
			GAN	0.28	0.25	0.22	0.22	0.21	0.20
			LightGBM	0.35	0.22	0.15	0.18	0.17	0.18
			Trans	0.64	0.41	0.29	0.22	0.15	0.13
			G-Trans	0.78	0.58	0.38	0.28	0.22	0.18
		F1 Score	RF	0.26	0.16	0.15	0.14	0.14	0.17
			SVM	0.25	0.25	0.22	0.21	0.21	0.19
			GAN	0.37	0.31	0.26	0.25 [†]	0.23*	0.21*
			LightGBM	0.36	0.25	0.22	0.24	0.19	0.21*
			Trans	0.70 [†]	0.45 [†]	0.30 [†]	0.22	0.16	0.13
			G-Trans	0.78*	0.58*	0.38*	0.28*	0.22 [†]	0.18
Cranberry, PA	I-76W	Recall	RF	0.01	-	-	-	-	-
			SVM	0.66	0.50	0.40	0.36	0.31	0.36
			GAN	0.53	0.38	0.29	0.29	0.30	0.29
			LightGBM	0.45	0.36	0.23	0.34	0.25	0.25
			Trans	0.58	0.45	0.31	0.27	0.23	0.20
			G-Trans	0.75	0.52	0.30	0.23	0.19	0.15
		Precision	RF	1.00	-	-	-	-	-
			SVM	0.08	0.06	0.05	0.05	0.04	0.05
			GAN	0.16	0.13	0.12	0.13	0.13	0.13
			LightGBM	0.16	0.12	0.18	0.07	0.13	0.17
			Trans	0.72	0.41	0.27	0.19	0.15	0.12
			G-Trans	0.76	0.53	0.31	0.24	0.19	0.15
		F1 Score	RF	0.02	-	-	-	-	-
			SVM	0.14	0.10	0.10	0.08	0.07	0.08
			GAN	0.25	0.20	0.17	0.18	0.18 [†]	0.18 [†]
			LightGBM	0.23	0.18	0.20	0.12	0.17	0.20*
			Trans	0.65 [†]	0.43 [†]	0.29 [†]	0.23 [†]	0.18 [†]	0.15
			G-Trans	0.76*	0.52*	0.30*	0.24*	0.19*	0.15
Cranberry, PA	I-76E	Recall	RF	0.05	0.03	0.07	0.10	0.10	0.10
			SVM	0.42	0.35	0.33	0.33	0.33	0.37
			GAN	0.34	0.23	0.20	0.23	0.27	0.27
			LightGBM	0.54	0.42	0.38	0.32	0.30	0.33
			Trans	0.74	0.44	0.15	0.08	0.08	0.08
			G-Trans	0.74	0.45	0.15	0.08	0.08	0.08
		Precision	RF	0.21	0.12	0.22	0.50	0.38	0.40
			SVM	0.08	0.07	0.06	0.06	0.06	0.07
			GAN	0.14	0.10	0.09	0.10	0.12	0.12
			LightGBM	0.10	0.08	0.07	0.07	0.06	0.07
			Trans	0.71	0.43	0.15	0.08	0.09	0.09
			G-Trans	0.72	0.41	0.14	0.08	0.08	0.08
		F1 Score	RF	0.08	0.05	0.10	0.17*	0.16*	0.16*
			SVM	0.14	0.11	0.11	0.10	0.10	0.10
			GAN	0.20	0.13	0.12	0.14 [†]	0.16*	0.16*
			LightGBM	0.16	0.13	0.11	0.11	0.10	0.11
			Trans	0.72*	0.43*	0.15*	0.08	0.09	0.09
			G-Trans	0.72*	0.43*	0.14 [†]	0.08	0.08	0.08
Cranberry, PA	US-29	Recall	RF	-	-	-	-	-	-
			SVM	0.47	0.36	0.39	0.39	0.45	0.51
			GAN	0.27	0.24	0.22	0.21	0.24	0.19
			LightGBM	0.11	0.16	0.13	0.11	0.13	0.09
			Trans	0.74	0.35	0.24	0.21	0.18	0.16
			G-Trans	0.77	0.54	0.31	0.22	0.19	0.16
		Precision	RF	-	-	-	-	-	-
			SVM	0.04	0.03	0.03	0.03	0.04	0.04
			GAN	0.06	0.06	0.05	0.05	0.05	0.04
			LightGBM	0.08	0.09	0.08	0.06	0.06	0.04
			Trans	0.76	0.61	0.47	0.44	0.40	0.35
			G-Trans	0.76	0.52	0.29	0.21	0.17	0.14
		F1 Score	RF	-	-	-	-	-	-
			SVM	0.08	0.06	0.06	0.06	0.07	0.08
			GAN	0.10	0.09	0.08	0.08	0.07	0.07
			LightGBM	0.09	0.11	0.10	0.08	0.08	0.06
			Trans	0.75 [†]	0.45 [†]	0.31*	0.28*	0.25*	0.22*
			G-Trans	0.77*	0.53*	0.30 [†]	0.21 [†]	0.18 [†]	0.15 [†]

Table 3: Cranberry Township Anomaly Detection/Prediction Results

Location		Model	DR	MTTD	FAR	DR(S)	MTTD(S)
County	Road						
Cranberry, PA	I-79S	OOD	0.14	0	0.99	0.00	-
		SVM	0.00	-	0.95	0.00	-
		GAN	0.00	-	0	0.00	-
		Ours	0.50	-1	0.08	1.00	-1
		Ours (a)	0.50	-12	0.00	1.00	-12
Cranberry, PA	I-79N	OOD	0.05	27	0.94	0.09	27
		SVM	0.21	14	0.94	0.18	30
		GAN	0.00	-	0	0.00	-
		Ours	0.58	-3	0.00	1.00	-3
		Ours (a)	0.57	-14	0.13	1.00	-14
Cranberry, PA	I-76W	OOD	0.33	14	0.99	0.33	14
		SVM	0.33	76	0.92	0.33	76
		GAN	0.33	76	0.77	0.33	76
		Ours	1.00	-2	0.00	1.00	-2
		Ours (a)	1.00	-17	0.10	1.00	-17
Cranberry, PA	I-76E	OOD	0.00	30	0.94	0.75	30
		SVM	0.00	27	0.89	1.00	27
		GAN	0.00	58	0.76	0.75	58
		Ours	0.80	-2	0.00	1.00	-2
		Ours (a)	0.80	-18	0.10	1.00	-18
Cranberry, PA	US-29	OOD	0.25	7	0.98	0.25	0
		SVM	0.78	5	0.95	1.00	5
		GAN	0.36	10	0.92	0.75	5
		Ours	0.44	-3	0.00	1.00	-3
		Ours (a)	0.44	-17	0.08	0.80	-17
Howard, MD	I-70E	OOD	0.00	-	1.00	0.00	-
		SVM	0.09	60	0.85	1.00	52
		GAN	0.61	1	0.10	1.00	2
		Ours	0.46	-7	0.00	1.00	-7
		Ours (a)	0.46	-12	0.23	1.00	-12
Howard, MD	I-70W	OOD	0.14	8	0.95	0.25	8
		SVM	0.71	33	0.95	1.00	25
		GAN	0.43	-14	0.2	0.75	-14
		Ours	0.57	-28	0.54	0.75	-6
		Ours (a)	0.28	-8	0.13	0.5	-8
Howard, MD	US-40E	OOD	0.00	-	1.00	0.00	-
		SVM	1.00	19	0.94	1.00	27
		GAN	0.67	2	0.00	0.80	2
		Ours	0.83	-17	0.00	1.00	-17
		Ours (a)	0.83	-42	0.00	1.00	-42
Howard, MD	US-40W	OOD	0.33	-7	0.40	0.40	-4
		SVM	0.67	0	0.88	0.80	0
		GAN	0.44	8	0.00	0.60	11
		Ours	0.56	-5	0.00	1.00	-5
		Ours (a)	0.44	-4	0.35	0.80	-4
Howard, MD	I-695A	OOD	0.00	-	0.96	0.00	-
		SVM	0.67	15	0.92	1.00	2
		GAN	0.67	-2	0.47	1.00	12
		Ours	0.22	-8	0.00	1.00	-8
		Ours (a)	0.22	-23	0.00	1.00	-23

Table 4: Overall performance of early anomaly detection/prediction

characteristics at 17:25. The model likely captured these characteristics and triggered the alert. This example demonstrates that our model successfully learned the early characteristics of incidents.

Appendix B and Figure 12 show our model’s predictions in a more complex scenario involving multiple incidents on 2023-01-25. In this example, our model also predicted the occurrence of the incidents earlier. This further demonstrates our model’s capability to effectively learn and identify early characteristics of incidents, even in more complex scenarios.

5.2.2 Examples of detecting anomalies and possibly unreported incidents

The above are two examples of direct prediction processes. During the periods mentioned, there were incident reports, and our model also issued alerts. However, there were also instances where no reports were present, but the alert was triggered (‘False Positive’ Cases), and cases where an incident report appeared later, but our model did not trigger an alert (‘False Negative’ Cases). Figures 13 and 14 illustrate these two kinds of cases, respectively.

Regarding false positive cases, we can observe in the four examples in Figure 13 that, despite no incident reports corresponding to the times on the dates indicated by the blue lines, there are clear anomalies when compared to recurrent patterns (represented by the orange and green dashed lines). Our model effectively captured these anomalies. As mentioned in the introduction, there is a significant missing issue with incident reports. These false alarms are likely due to the absence of incident reports, which underscores the importance of training with anomaly labels rather than relying solely on incident reports.

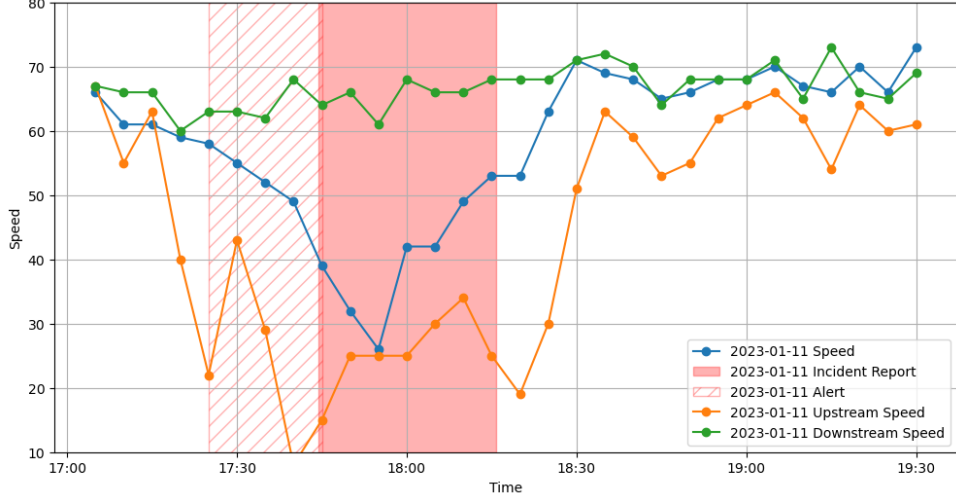


Figure 11: Upstream and Downstream speed on 2023-01-11

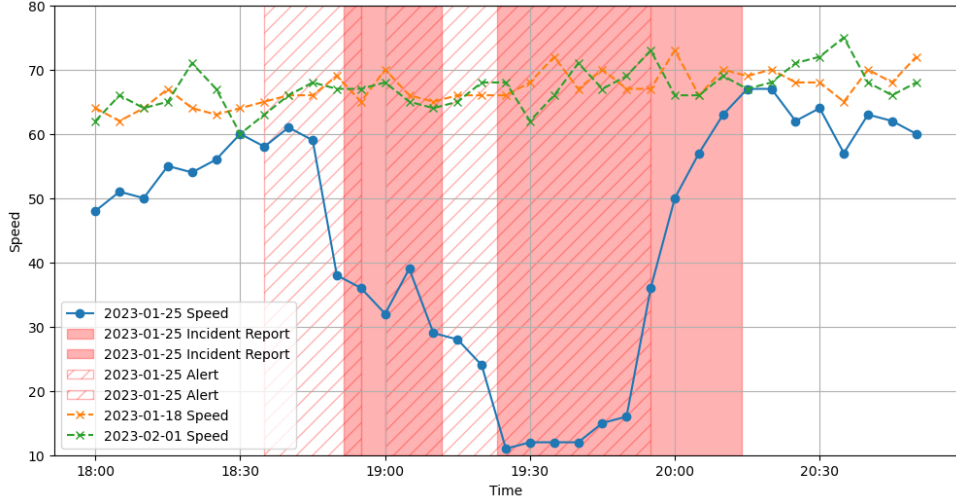


Figure 12: Speed, Alert, and Incident Report on 2023-01-25

Regarding false negative cases, from Figure 14, we can observe that compared to the recurrent pattern, the speed during the incident report period does not show significant changes, and most of these cases occur during non-peak hours. This could be because the incident reports are false, or do not have a significant impact, making it difficult for our model to detect them.

5.2.3 Overall Results

The above are specific case analyses. To demonstrate the generalizability of our model, Table 4 shows the testing results for 10 segments across two road networks. The metrics used are defined as follows:

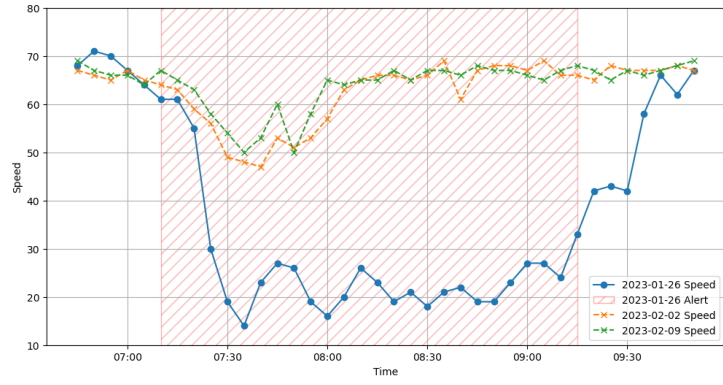
$$\text{DR (Detection Rate)} = \frac{N_{\text{detected_incident}}}{N_{\text{incident_report}}} \quad (11)$$

$$\text{MTTD (Mean Time to Detection)} = \frac{\sum_{i=1}^{N_{\text{detected_incident}}} (t_i^{\text{alarm}} - t_i^{\text{report}})}{N_{\text{detected_incident}}} \quad (12)$$

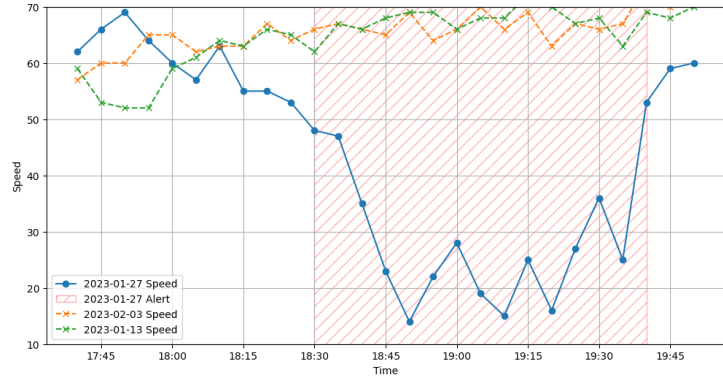
$$\text{FAR (False Alarm Rate)} = \frac{N_{\text{non-incident-non-anomaly}}}{N_{\text{alarm}}} \quad (13)$$

$$\text{DR (S) (Detection Rate, Significant)} = \frac{N_{\text{detected_significant_incident}}}{N_{\text{significant_incident_report}}} \quad (14)$$

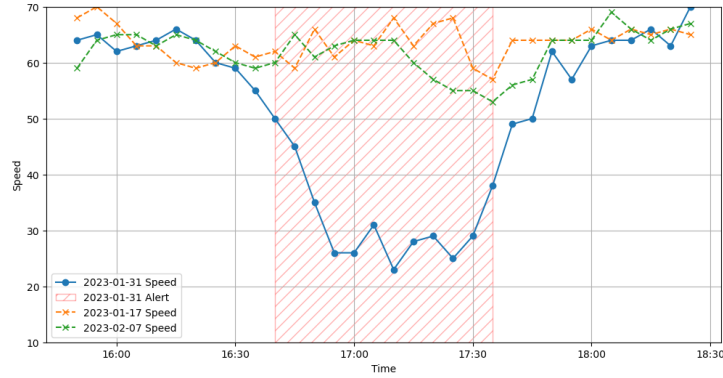
$$\text{MTTD (S) (Mean Time to Detection, Significant)} = \frac{\sum_{i=1}^{N_{\text{detected_significant_incident}}} (t_i^{\text{alarm}} - t_i^{\text{report}})}{N_{\text{detected_significant_incident}}} \quad (15)$$



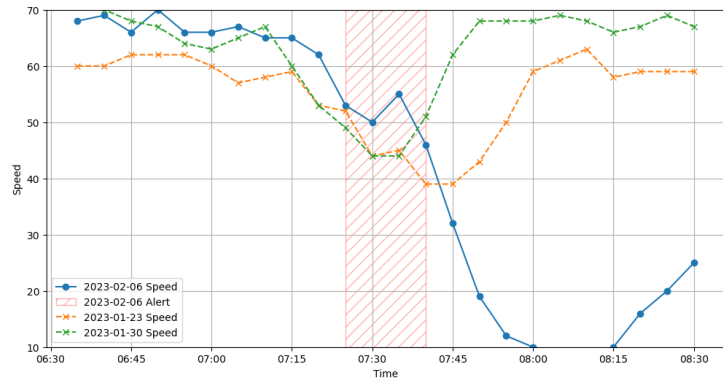
(a) 2023-01-26 Case



(b) 2023-01-27 Case

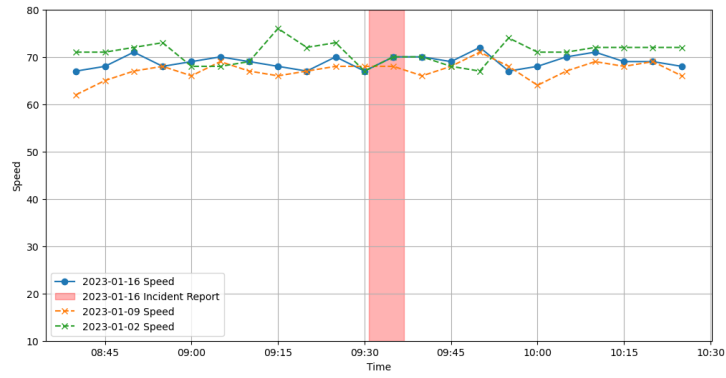


(c) 2023-01-31 Case

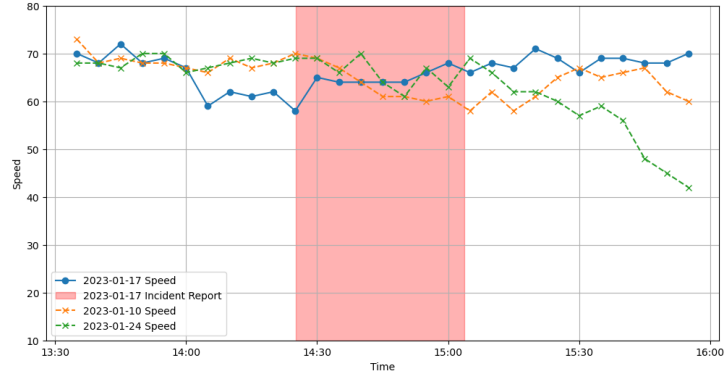


(d) 2023-02-06 Case

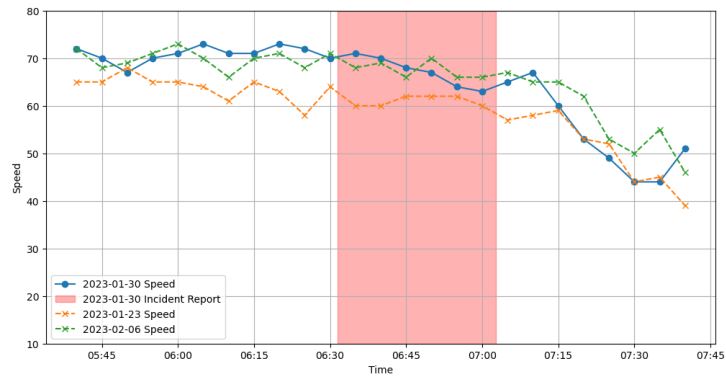
Figure 13: The 'False Positive' Cases



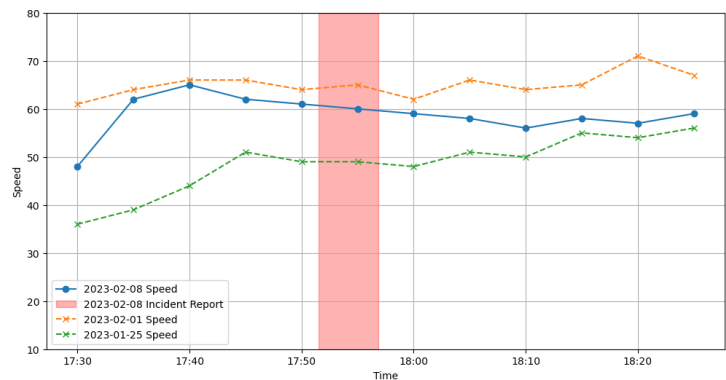
(a) 2023-01-16 Case



(b) 2023-01-17 Case



(c) 2023-01-30 Case



(d) 2023-02-08 Case

Figure 14: The 'False Negative' Cases

The definitions of DR and MTTD are generally consistent with those used in other studies. The definition of detected incidents in Equation 11 is as follows: from the start to the end of an incident report, if the model triggers an alert during this period, it is considered detected. Note that detection after the report start time is typically less helpful if the incident has been reported to an operator. In Equation 12, t_i^{report} refers to the start time of the report, and t_i^{alarm} refers to the time when the model begins to trigger an alert. If there are multiple continuous alerts within one incident report, the earliest one is taken. Considering the incident report is typically after the actual (possibly unknown) occurrence time, negative values are allowed when calculating MTTD and indicate early detection/prediction.

Considering the issues caused by incident missing report, as shown in Figures 3 and 13, we have optimized the definition of FAR (False Alarm Rate) in Equation 13. The numerator of FAR has been changed from the number of alarms not coinciding with any incident reports to the number of alarms not coinciding with any incident reports or anomalies. The anomalies here are those generated using the anomaly labels described in Section 4.2. This adjustment reduces the likelihood of alarms that captured anomalies, such as those in Figure 13, being classified as false alarms.

The settings for DR (Significant) and MTTD (Significant) in Equations 14 and 15 aim to exclude the interference of some false reports or insignificant incidents in the evaluation process. A significant incident is defined as any incident that overlaps with our generated anomaly labels, i.e., the incidents retained in Step 1 of Algorithm 1. The other calculation principles are consistent with those in Equations 11 and 1.

We adopted the following conventional AID baselines. It is important to note that, as we have already demonstrated the effectiveness of training with anomaly labels in the previous chapter, and since almost all existing studies use incident reports for training, all the baselines here, except for the first one whose detection process is based on statistical methods, are trained using incident reports. Given the differences in input data, for example, we do not have loop detector data, we cannot directly use the original baseline models. However, we have made efforts to retain the proposed model’s structure and adapt it by tuning it to our dataset.

- **OOD**, Out of Distribution. OOD is based on the statistical method. we use the Seq2Seq with attention model (Bahdanau et al., 2014) to train speed predictions until convergence. The model will trigger an alert by measuring the SND (Standardized Normal Deviate) between observed and predicted values. The SND threshold is tuned based on the incidence rate of the incident reports.
- **SVM**, Support Vector Machine. We train a binary classification SVM with an RBF kernel based on whether there is an incident report in the next time step.
- **GAN**, Generative Adversarial Network. We first use a GAN (Generative Adversarial Network) to learn the characteristics of samples with incident reports and generate some fake samples. These fake samples, along with the real samples, are used to train the SVM.
- **Ours**. Our model trained without ahead-labelled anomaly labels
- **Ours (a)**. Our model trained with 15-minute ahead-labelled anomaly labels

In Table 4, we first crossed out some results that lack practical significance, such as extremely high FAR or cases where both DR and DR(S) are 0. The reasons for crossed out are marked in red.

Our model achieved a low FAR overall while obtaining high DR and low MTTD, especially with DR(S) almost all being 1. This is naturally related to our model is trained by anomaly labels and reflects that our model has successfully detected the incidents marked as significant. Furthermore, even without ahead labeling, all our MTTD values are negative, indicating detection before the incident reports. This shows that the addition of anomaly samples has already incorporated features that precede the incident reports.

After ahead labeling, our model further reduced MTTD in 8 out of 10 cases, demonstrating the significance of ahead labeling. In most cases, DR remained unchanged, but FAR generally increased slightly, though still within an acceptable low range. This is reasonable, as the ahead labeling process can label some non-anomaly samples as anomalies. For the I-79S case where DR, FAR, and MTTD all worsened, we may need to reduce the ahead labeling time θ_{ahead} to prevent the inclusion of too many non-anomaly samples.

Among baseline methods, OOD only shows some practical significance in Howard County US-40, while other results face very high FAR and low DR. Notably, they all converge well in the speed prediction model. This highlights the drawbacks of statistical methods, where outliers in SND are not necessarily anomalies but could be due to model prediction errors and probe vehicle speed observation errors. Although statistical methods have performed well in some studies, probe vehicle data may still be too noisy to support this method. Regarding SVM, the results of the SVM are entirely lacking in practical significance. This may be due to the difficulty in learning from incident reports. Because when we trained using anomaly labels (See Tables 2 and 3), they achieved convergence in most cases.

GAN achieved good convergence across all cases in Howard County. This may be because GAN learned the anomaly characteristics from the incident reports, and its generator produced samples similar to those we

generated using Algorithm 1. By using incident reports directly for training, the DR of GAN in I-70E and I-695A was higher than our method, although their FAR was also relatively high. Overall, GAN’s MTTD was still worse than our method, reflecting the lack of early features in the incident reports. In addition, GAN performed poorly in Cranberry Township, even worse than SVM in I-79S and I-79N, indicating that the samples generated by GAN actually added noise. This suggests that GAN still struggles to learn incident characteristics in the Cranberry Map. In the future, we might consider using prior knowledge, such as slowdown speed, to guide the learning process of GAN.

6 Conclusion and Future Work

In this study, we address an early anomaly detection or prediction problem that is more practically useful and scalable than conventional AID models. We propose a method that combines incident reports and traffic domain knowledge, i.e., the correlation between slowdown speed and incident, to generate anomaly labels and train a deep learning model for early anomaly detection. This method aims to overcome inherent issues in incident reports, including false reports, insignificant incident reports, delayed reports, and missing reports. We adopted ahead labeling and multi-step prediction strategies, allowing the model to predict incidents earlier than traditional methods. Additionally, we applied various machine learning strategies to address the issues of insufficient anomaly samples and data imbalance. Unlike existing research in the field of AID, our method aims to capture a broader range of anomalies beyond *after the fact* incident reports (including early incident characteristics and unreported anomalies) and more importantly, offer early alerts of anomalies that potentially influence the traffic flow in the short term. Furthermore, our method is highly scalable as it relies solely on ubiquitously available data. We validated our model on ten road sections in two road networks, achieving results that surpassed the baselines. This experiment shows a good trade-off between precision and recall, and resulting anomaly alerts 4-42 min earlier than Waze reports.

Although the data used in this study is theoretically available in real-time, we need to coordinate with data providers to ensure we can access the real-time data required by the model as early as possible. This will maximize the model’s advantage in early prediction/detection for potential future applications. Besides, this study also has certain limitations that can be improved. First, regarding the selection of prior knowledge, we mainly chose edges with a high correlation between the occurrence of incidents and high slowdown speeds. In fact, due to the topological structure, not all edges have this correlation. Bases on our definition of slowdown speed, this high correlation requires that the segment be relatively long and that most incidents do not occur at the very beginning of each segment. For those that do not exhibit this high correlation, we may need to consider redefining the slowdown speed or using other values, such as the travel time index. Semi-supervised learning is also a potential solution for label denoising. Moreover, our algorithm is also difficult to handle for segments where only one or two incidents occur per year, as the validation and test sets may not contain any incidents. This might require using simulator data to generate sufficient training samples and finetuning with real-world incident samples. Additionally, we can tune a reasonable ahead-labeling period, which is also a direction worth exploring in future research.

Acknowledgement

This research is supported by US Department of Transportation Exploratory Advanced Research Award 693JJ321C000013. The contents of this paper reflect the views of the authors only, who are responsible for the facts and the accuracy of the information presented herein.

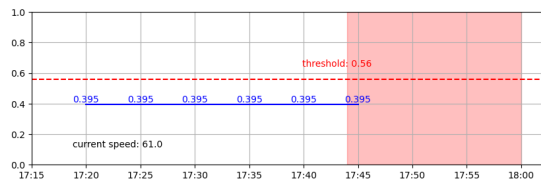
References

- Abdulhai, B., & Ritchie, S. G. (1999). Enhancing the universality and transferability of freeway incident detection using a bayesian-based neural network. *Transportation Research Part C: Emerging Technologies*, 7(5), 261–280.
- Ahmed, F., & Hawas, Y. (2015). An integrated real-time traffic signal system for transit signal priority, incident detection and congestion management. *Transportation Research Part C: Emerging Technologies*, 60, 52–76.
- Ahmed, S. A., & Cook, A. R. (1982). Application of time-series analysis techniques to freeway incident detection. *Transportation Research Record*, 841(3), 19–21.
- Asakura, Y., Kusakabe, T., Nguyen, L. X., & Ushiki, T. (2017). Incident detection methods using probe vehicles with on-board gps equipment. *Transportation research part C: emerging technologies*, 81, 330–341.
- Bahdanau, D., Cho, K., & Bengio, Y. (2014). Neural machine translation by jointly learning to align and translate. *arXiv preprint arXiv:1409.0473*.
- Balke, K., Dudek, C. L., & Mountain, C. E. (1996). Using probe-measured travel times to detect major freeway incidents in houston, texas. *Transportation Research Record*, 1554(1), 213–220.
- Chakraborty, P., Hegde, C., & Sharma, A. (2019). Data-driven parallelizable traffic incident detection using spatio-temporally denoised robust thresholds. *Transportation research part C: emerging technologies*, 105, 81–99.
- Chakraborty, P., Sharma, A., & Hegde, C. (2018). Freeway traffic incident detection from cameras: A semi-supervised learning approach. In *2018 21st international conference on intelligent transportation systems (itsc)* (pp. 1840–1845).
- Cheu, R. L., & Ritchie, S. G. (1995). Automated detection of lane-blocking freeway incidents using artificial neural networks. *Transportation Research Part C: Emerging Technologies*, 3(6), 371–388.
- Cheu, R. L., & Tay, G. C. W. (2004). Sampling strategies for probe-vehicle-based freeway incident detection algorithms. *Transportation research record*, 1867(1), 80–88.
- Dia, H., & Rose, G. (1997). Development and evaluation of neural network freeway incident detection models using field data. *Transportation Research Part C: Emerging Technologies*, 5(5), 313–331.
- Dudek, C. L., Messer, C. J., & Nuckles, N. B. (1974). Incident detection on urban freeways. *Transportation research record*, 495, 12–24.
- ElSahly, O., & Abdelfatah, A. (2022). A systematic review of traffic incident detection algorithms. *Sustainability*, 14(22), 14859.
- Federal Highway Administration (FHWA). (2020a). *Process for establishing, implementing, and institutionalizing a traffic incident management performance measurement program*. <https://ops.fhwa.dot.gov/publications/fhwahop15028/step1.htm>.
- Federal Highway Administration (FHWA). (2020b). *Traffic congestion and reliability: Trends and advanced strategies for congestion mitigation* (Tech. Rep.). Federal Highway Administration (FHWA). Retrieved from https://ops.fhwa.dot.gov/congestion_report/executive_summary.htm (Accessed: 2023-04-21)
- Goodfellow, I., Pouget-Abadie, J., Mirza, M., Xu, B., Warde-Farley, D., Ozair, S., ... Bengio, Y. (2014). Generative adversarial nets. *Advances in neural information processing systems*, 27.
- Gu, Y., Qian, Z. S., & Chen, F. (2016). From twitter to detector: Real-time traffic incident detection using social media data. *Transportation research part C: emerging technologies*, 67, 321–342.
- Han, X., Grubenmann, T., Cheng, R., Wong, S. C., Li, X., & Sun, W. (2020). Traffic incident detection: A trajectory-based approach. In *2020 IEEE 36th International Conference on Data Engineering (ICDE)* (pp. 1866–1869).
- Hastie, T., Tibshirani, R., Friedman, J. H., & Friedman, J. H. (2009). *The elements of statistical learning: data mining, inference, and prediction* (Vol. 2). Springer.
- Jin, X., Cheu, R. L., & Srinivasan, D. (2002). Development and adaptation of constructive probabilistic neural network in freeway incident detection. *Transportation Research Part C: Emerging Technologies*, 10(2), 121–147.
- Karim, A., & Adeli, H. (2002). Incident detection algorithm using wavelet energy representation of traffic patterns. *Journal of Transportation Engineering*, 128(3), 232–242.
- Ke, G., Meng, Q., Finley, T., Wang, T., Chen, W., Ma, W., ... Liu, T.-Y. (2017). Lightgbm: A highly efficient gradient boosting decision tree. *Advances in neural information processing systems*, 30.

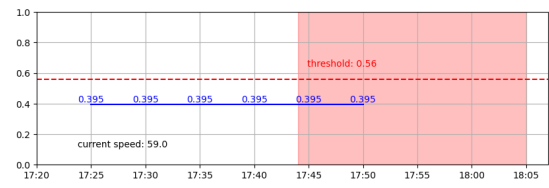
- Ke, Z., Duan, H., & Qian, S. (2024). Interpretable mixture of experts for time series prediction under recurrent and non-recurrent conditions. *arXiv preprint arXiv:2409.03282*.
- Ke, Z., Zou, Q., Liu, J., & Qian, S. (2024). Real-time system optimal traffic routing under uncertainties—can physics models boost reinforcement learning? *arXiv preprint arXiv:2407.07364*.
- Ki, Y.-K., & Lee, D.-Y. (2007). A traffic accident recording and reporting model at intersections. *IEEE Transactions on Intelligent Transportation Systems*, 8(2), 188–194.
- Li, L., Lin, Y., Du, B., Yang, F., & Ran, B. (2022). Real-time traffic incident detection based on a hybrid deep learning model. *Transportmetrica A: transport science*, 18(1), 78–98.
- Lin, Y., Li, L., Jing, H., Ran, B., & Sun, D. (2020). Automated traffic incident detection with a smaller dataset based on generative adversarial networks. *Accident Analysis & Prevention*, 144, 105628.
- Pan, D. (2022). *Development of incident detection algorithms compatible with low temporal-resolution traffic detectors and limited incident data* (Unpublished doctoral dissertation). The George Washington University.
- Parkany, E., & Xie, C. (2005). *A complete review of incident detection algorithms & their deployment: What works and what doesn't* (Technical Report No. NETCR37). New England Transportation Consortium. Retrieved from <https://onlinepubs.trb.org/onlinepubs/trispdfs/00988875.pdf>
- Payne, H. J., & Tignor, S. C. (1978). Freeway incident-detection algorithms based on decision trees with states. *Transportation Research Record*(682).
- Persaud, B. N., & Hall, F. L. (1989). Catastrophe theory and patterns in 30-second freeway traffic data—implications for incident detection. *Transportation Research Part A: General*, 23(2), 103–113.
- Petty, K. F., Noeimi, H., Sanwal, K., Rydzewski, D., Skabardonis, A., Varaiya, P., & Al-Deek, H. (1996). The freeway service patrol evaluation project: Database support programs, and accessibility. *Transportation Research Part C: Emerging Technologies*, 4(2), 71–85.
- Sermons, M. W., & Koppelman, F. S. (1996). Use of vehicle positioning data for arterial incident detection. *Transportation Research Part C: Emerging Technologies*, 4(2), 87–96.
- Sethi, V., Bhandari, N., Koppelman, F. S., & Schofer, J. L. (1995). Arterial incident detection using fixed detector and probe vehicle data. *Transportation Research Part C: Emerging Technologies*, 3(2), 99–112.
- Sheu, J.-B. (2002). A stochastic optimal control approach to real-time, incident-responsive traffic signal control at isolated intersections. *Transportation Science*, 36(4), 418–434.
- Singh, D., & Mohan, C. K. (2018). Deep spatio-temporal representation for detection of road accidents using stacked autoencoder. *IEEE Transactions on Intelligent Transportation Systems*, 20(3), 879–887.
- Stephanedes, Y. J., & Chassiakos, A. P. (1993). Application of filtering techniques for incident detection. *Journal of transportation engineering*, 119(1), 13–26.
- Sutskever, I., Vinyals, O., & Le, Q. V. (2014). Sequence to sequence learning with neural networks. *Advances in neural information processing systems*, 27.
- Turner, B., Breen, J., & Howard, E. (2015). *Road safety manual: a manual for practitioners and decision makers on implementing safe system infrastructure*. <https://roadsafety.piarc.org/en/road-safety-management-safety-data/quality-and-under-reporting>.
- Vapnik, V. (2013). *The nature of statistical learning theory*. Springer science & business media.
- Vaswani, A., Shazeer, N., Parmar, N., Uszkoreit, J., Jones, L., Gomez, A. N., . . . Polosukhin, I. (2017). Attention is all you need. *Advances in neural information processing systems*, 30.
- Williams, R. J., & Zipser, D. (1989). A learning algorithm for continually running fully recurrent neural networks. *Neural computation*, 1(2), 270–280.
- Wirasinghe, S. C. (1978). Determination of traffic delays from shock-wave analysis. *Transportation Research*, 12(5), 343–348.
- Wu, Z., Jain, P., Wright, M., Mirhoseini, A., Gonzalez, J. E., & Stoica, I. (2021). Representing long-range context for graph neural networks with global attention. *Advances in Neural Information Processing Systems*, 34, 13266–13279.
- Xie, Q., Guo, T., Chen, Y., Xiao, Y., Wang, X., & Zhao, B. Y. (2020). Deep graph convolutional networks for incident-driven traffic speed prediction. In *Proceedings of the 29th acm international conference on information & knowledge management* (pp. 1665–1674).
- Yao, W., & Qian, S. (2020). Learning to recommend signal plans under incidents with real-time traffic prediction. *Transportation Research Record*, 2674(6), 45–59. Retrieved from <https://doi.org/10.1177/0361198120917668> DOI: 10.1177/0361198120917668

- Yuan, F., & Cheu, R. L. (2003). Incident detection using support vector machines. *Transportation Research Part C: Emerging Technologies*, 11(3-4), 309–328.
- Zhang, Z., He, Q., Gao, J., & Ni, M. (2018). A deep learning approach for detecting traffic accidents from social media data. *Transportation research part C: emerging technologies*, 86, 580–596.

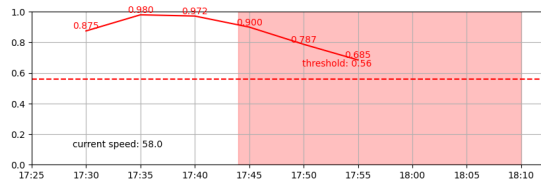
A Prediction/Detection Example on 2023-01-11



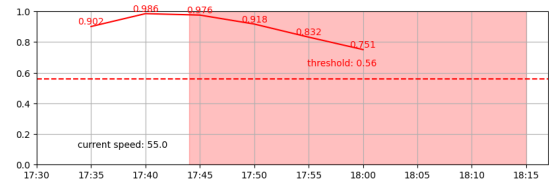
Prediction at 2023-01-11 17:15



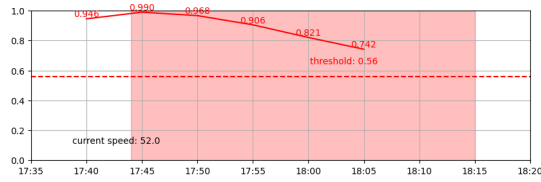
Prediction at 2023-01-11 17:20



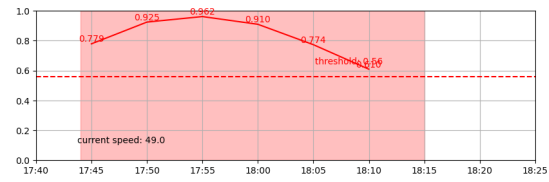
Prediction at 2023-01-11 17:25



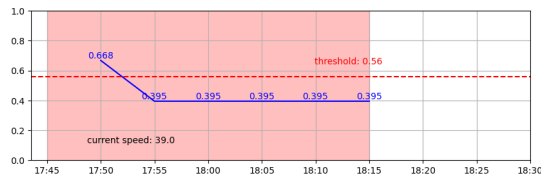
Prediction at 2023-01-11 17:30



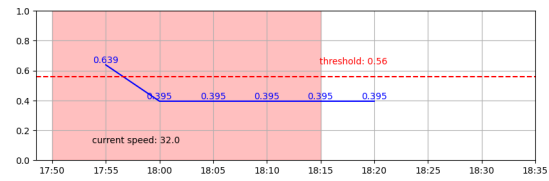
Prediction at 2023-01-11 17:35



Prediction at 2023-01-11 17:40

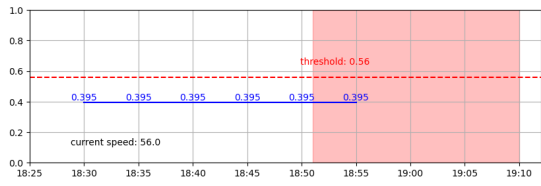


Prediction at 2023-01-11 17:45

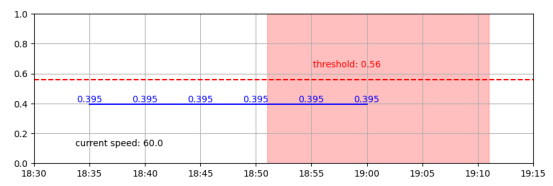


Prediction at 2023-01-11 17:50

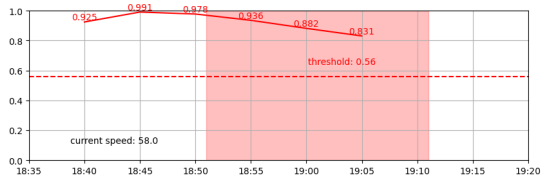
B Prediction/Detection Example on 2023-01-25



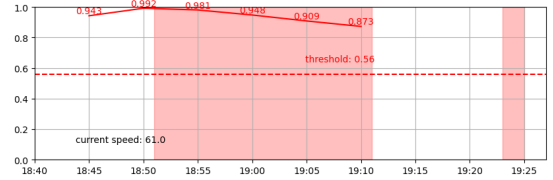
Prediction at 2023-01-25 18:25



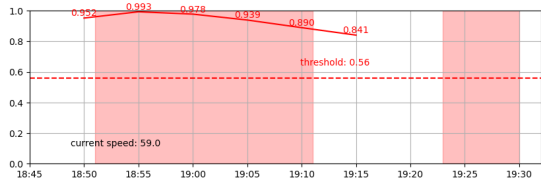
Prediction at 2023-01-25 18:30



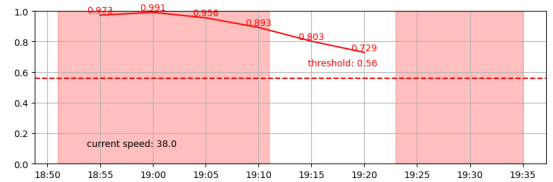
Prediction at 2023-01-25 18:35



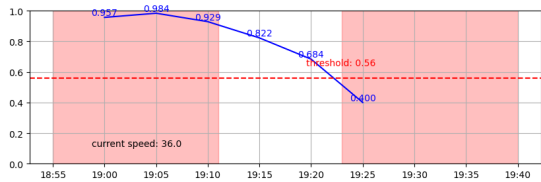
Prediction at 2023-01-25 18:40



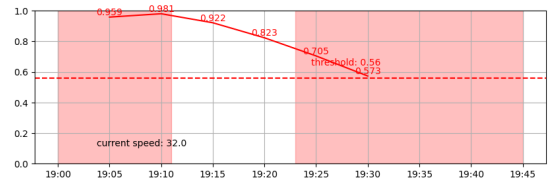
Prediction at 2023-01-25 18:45



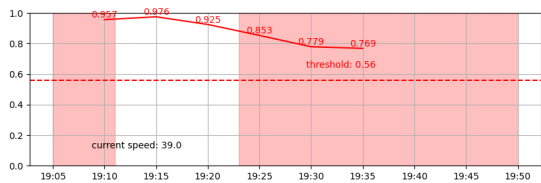
Prediction at 2023-01-25 18:50



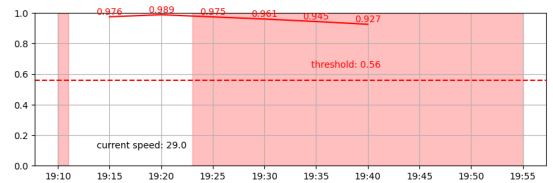
Prediction at 2023-01-25 18:55



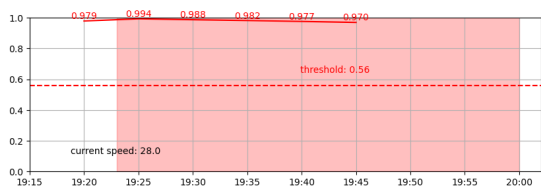
Prediction at 2023-01-25 19:00



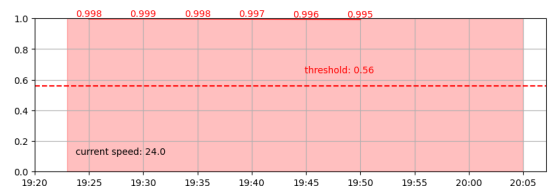
Prediction at 2023-01-25 19:05



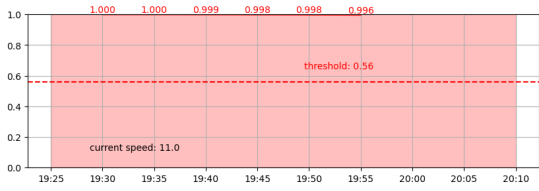
Prediction at 2023-01-25 19:10



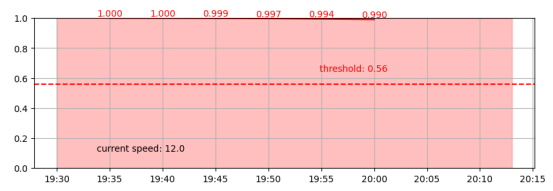
Prediction at 2023-01-25 19:15



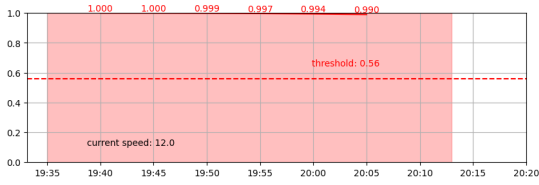
Prediction at 2023-01-25 19:20



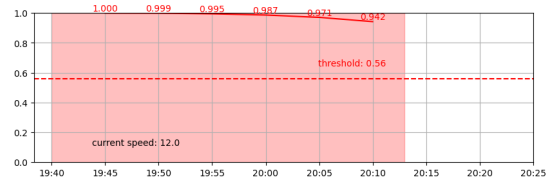
Prediction at 2023-01-25 19:25



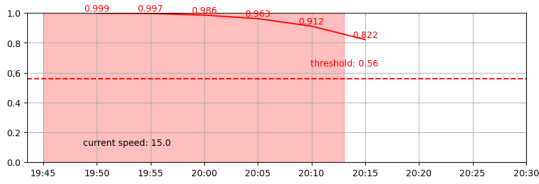
Prediction at 2023-01-25 19:30



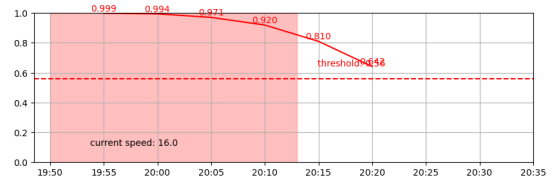
Prediction at 2023-01-25 19:35



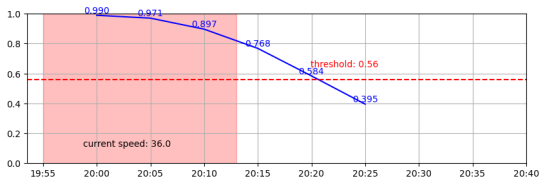
Prediction at 2023-01-25 19:40



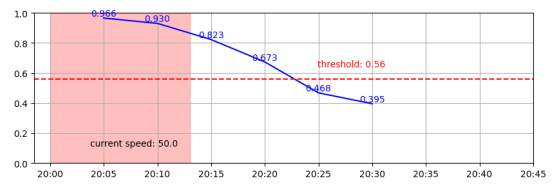
Prediction at 2023-01-25 19:45



Prediction at 2023-01-25 19:50



Prediction at 2023-01-25 19:55



Prediction at 2023-01-25 20:00